



HAL
open science

TNF- α and α -synuclein fibrils differently regulate human astrocyte immune reactivity and impair mitochondrial respiration

Kaspar Russ, Gabriel Teku, Luc Bousset, Virginie Redeker, Sara Piel, Ekaterina Savchenko, Yuriy Pomeschchik, Jimmy Savistchenko, Tina C Stummann, Carla Azevedo, et al.

► To cite this version:

Kaspar Russ, Gabriel Teku, Luc Bousset, Virginie Redeker, Sara Piel, et al.. TNF- α and α -synuclein fibrils differently regulate human astrocyte immune reactivity and impair mitochondrial respiration. Cell Reports, 2021, 34 (12), pp.108895. 10.1016/j.celrep.2021.108895 . cea-03186002

HAL Id: cea-03186002

<https://cea.hal.science/cea-03186002>

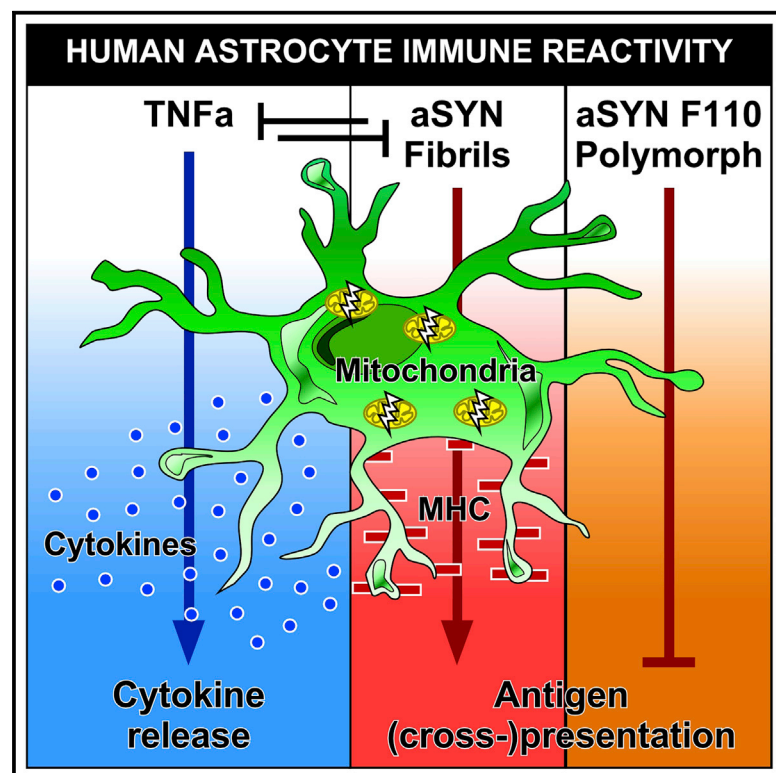
Submitted on 30 Mar 2021

HAL is a multi-disciplinary open access archive for the deposit and dissemination of scientific research documents, whether they are published or not. The documents may come from teaching and research institutions in France or abroad, or from public or private research centers.

L'archive ouverte pluridisciplinaire **HAL**, est destinée au dépôt et à la diffusion de documents scientifiques de niveau recherche, publiés ou non, émanant des établissements d'enseignement et de recherche français ou étrangers, des laboratoires publics ou privés.

TNF- α and α -synuclein fibrils differently regulate human astrocyte immune reactivity and impair mitochondrial respiration

Graphical abstract



Authors

Kaspar Russ, Gabriel Teku, Luc Bousset, ..., Mauno Vihinen, Ronald Melki, Laurent Roybon

Correspondence

laurent.roybon@med.lu.se

In brief

Russ et al. show that human astrocytes adopt different reactive immune phenotypes when exposed to either TNF- α or alpha-synuclein fibrils, which are exogenous stressors that compete to drive the astrocyte immune reactive response. They also show that *PARK2*-variant-containing astrocytes exhibit an exacerbated response to the stressors, accompanied by bioenergetic defects.

Highlights

- Astrocytes exposed to TNF- α , but not α SYN fibrils, release pro-inflammatory cytokines
- Astrocytes exposed to α SYN fibrils become antigen (cross)-presenting cells
- Antigen (cross) presentation is hampered by large F110 fibrils
- Astrocytes exposed to TNF- α or α SYN fibrils have impaired mitochondrial respiration



Report

TNF- α and α -synuclein fibrils differently regulate human astrocyte immune reactivity and impair mitochondrial respiration

Kaspar Russ,^{1,2,9} Gabriel Teku,^{3,11} Luc Bousset,^{4,11} Virginie Redeker,^{4,12} Sara Piel,^{5,10,12} Ekaterina Savchenko,^{1,2} Yuriy Pomeschchik,^{1,2} Jimmy Savistchenko,⁴ Tina C. Stummann,⁸ Carla Azevedo,^{1,2} Anna Collin,⁶ Stefano Goldwurm,⁷ Karina Fog,⁸ Eskil Elmer,⁵ Mauno Vihinen,³ Ronald Melki,^{4,13} and Laurent Roybon^{1,2,13,14,*}

¹Cell Stem Cell Laboratory for CNS Disease Modeling, Department of Experimental Medical Science, BMC D10, Lund University, 22184 Lund, Sweden

²MultiPark and the Lund Stem Cell Center, Lund University, 22184 Lund, Sweden

³Protein Structure and Bioinformatics, Department of Experimental Medical Science, BMC B13, Lund University, 22184 Lund, Sweden

⁴Institut Francois Jacob (MIRcen), CEA and Laboratory of Neurodegenerative Diseases, CNRS, 18 Route du Panorama, 92265 Fontenay-Aux-Roses, France

⁵Mitochondrial Medicine, Department of Clinical Sciences Lund, Lund University, 22184 Lund, Sweden

⁶Office for Medical Services/division of Laboratory Medicine, Department of Clinical Genetics and Pathology, Lund, Sweden

⁷Centro Parkinson/Parkinson Institute, ASST "Gaetano Pini/CTO," via Bignami 1, 20126 Milan, Italy

⁸H. Lundbeck A/S, Valby, Denmark

⁹Present address: H. Lundbeck A/S, Valby, Denmark

¹⁰Present address: Center for Mitochondrial and Epigenomic Medicine, Department of Anesthesiology and Critical Care Medicine, Children's Hospital of Philadelphia, Philadelphia, PA 19104-4302, USA

¹¹These authors contributed equally

¹²These authors contributed equally

¹³Senior author

¹⁴Lead contact

*Correspondence: laurent.roybon@med.lu.se
<https://doi.org/10.1016/j.celrep.2021.108895>

SUMMARY

Here, we examine the cellular changes triggered by tumor necrosis factor alpha (TNF- α) and different alpha-synuclein (α SYN) species in astrocytes derived from induced pluripotent stem cells. Human astrocytes treated with TNF- α display a strong reactive pro-inflammatory phenotype with upregulation of pro-inflammatory gene networks, activation of the nuclear factor κ B (NF- κ B) pathway, and release of pro-inflammatory cytokines, whereas those treated with high-molecular-weight α SYN fibrils acquire a reactive antigen (cross)-presenting phenotype with upregulation of major histocompatibility complex (MHC) genes and increased human leukocyte antigen (HLA) molecules at the cell surface. Surprisingly, the cell surface location of MHC proteins is abrogated by larger F110 fibrillar polymorphs, despite the upregulation of MHC genes. Interestingly, TNF- α and α SYN fibrils compete to drive the astrocyte immune reactive response. The astrocyte immune responses are accompanied by an impaired mitochondrial respiration, which is exacerbated in Parkinson's disease (PD) astrocytes. Our data provide evidence for astrocytic involvement in PD pathogenesis and reveal their complex immune reactive responses to exogenous stressors.

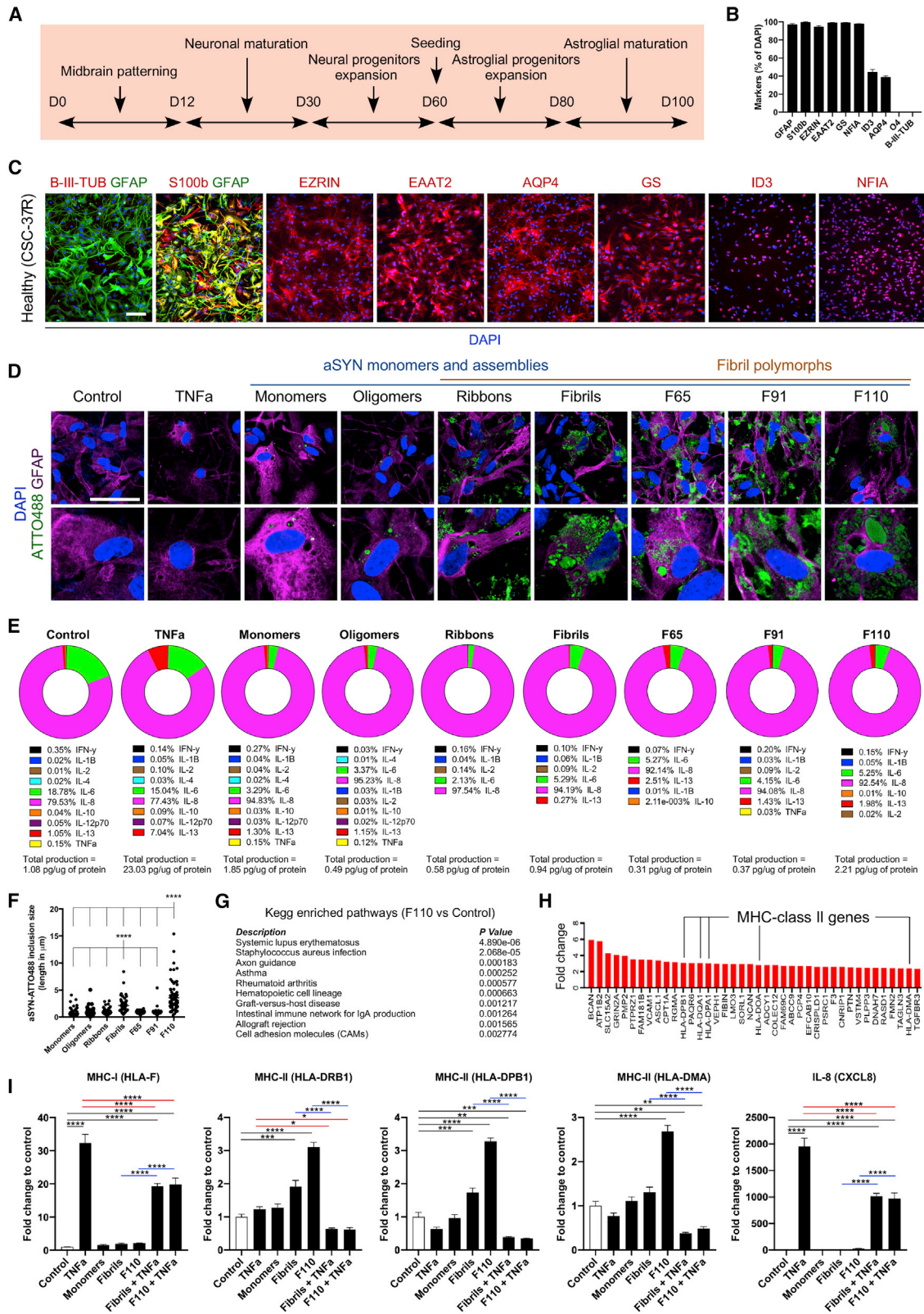
INTRODUCTION

Parkinson's disease (PD) is a multifactorial neurodegenerative disorder characterized, in part, by the death of pigmented midbrain dopaminergic neurons located in the *substantia nigra pars compacta* (SNpc), resulting in motor and non-motor dysfunctions that are prominent at advanced disease stages (Poewe et al., 2017). The major neuropathological characteristics of PD are the presence of alpha-synuclein (α SYN)-containing Lewy bodies in injured neurons and neuroinflammation in the SNpc (Spillantini et al., 1997, 1998).

α SYN is a 14-kDa protein encoded by the SNCA gene, which under disease conditions can oligomerize into a wide range of high-molecular-weight (MW) oligomers, of which some are fibrillar in nature. They have well-defined structures and properties and exhibit distinct seeding and propagation propensities *in vivo* (Bousset et al., 2013; Guerrero-Ferreira et al., 2019; Li et al., 2018; Makky et al., 2016; Peelaerts et al., 2015; Sun et al., 2020).

α SYN has been observed in immune reactive astrocytes in PD patients' brains (Braak et al., 2007). However, it is not known how different α SYN species that may be present in the PD brain can





(legend on next page)

influence glial immune reactivity and function. Answering this question would provide invaluable insight into how α SYN, inflammation, and astrocytes interact in PD pathogenesis. Moreover, because astrocytes express PD-linked genes at levels sometimes similar to neurons (Booth et al., 2017; Zhang et al., 2016), they are expected to exhibit more profound cellular changes than healthy astrocytes, when exposed to aggregated α SYN polymorphs. Such changes might ultimately impact the survival of the neurons they support, particularly dopaminergic neurons.

Uptake of α SYN by rodent astrocytes from neuronally differentiated SH-SY5Y cells overexpressing SNCA induced astrocytic expression of genes related to an immune reactive response (Lee et al., 2010). However, it remains to be determined which component of the immune reactive state of the astrocytes was triggered by α SYN, among the factors secreted in response to SNCA overexpression. This information would be valuable for the development of therapeutic strategies.

In this study, we investigated whether and how different α SYN species induce human astrocyte immune reactivity.

RESULTS

Human iPSC-derived astrocytes exposed to high-MW α SYN species do not release pro-inflammatory cytokines but adopt an antigen (cross)-presenting phenotype

In order to investigate the effect of α SYN species on human astrocytic immune reactivity, we generated induced pluripotent stem cells (iPSCs) from fibroblasts of two non-demented healthy donors (Figure S1). We differentiated iPSCs into astrocytes by using a protocol that spans 100 days (Figure 1A), which was modified from our previous work (Holmqvist et al., 2015). The cells had an astrocytic morphology and the majority stained positive for canonical astrocyte markers GFAP, S100b, EZRIN, EAAT2, AQP4, GS, ID3, and NFIA (Figures 1B and 1C).

First, we confirmed that the astrocytes generated could become immune reactive pro-inflammatory, following treatment with tumor necrosis factor alpha (TNF- α) (Roybon et al., 2013). Human iPSC-derived astrocytes were treated for 6 days with

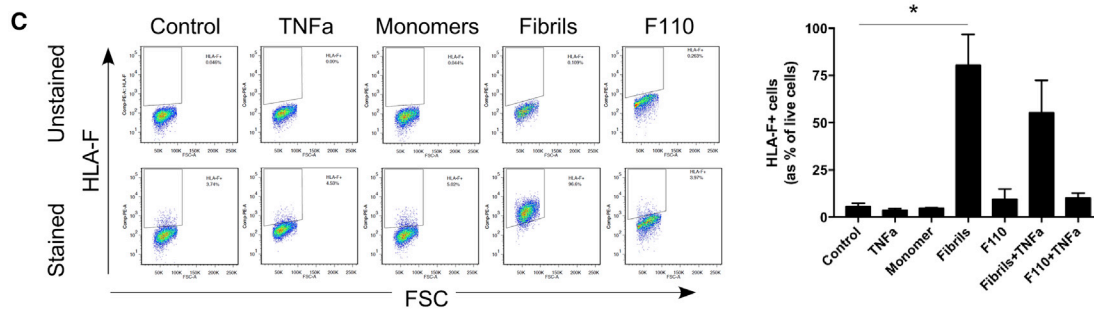
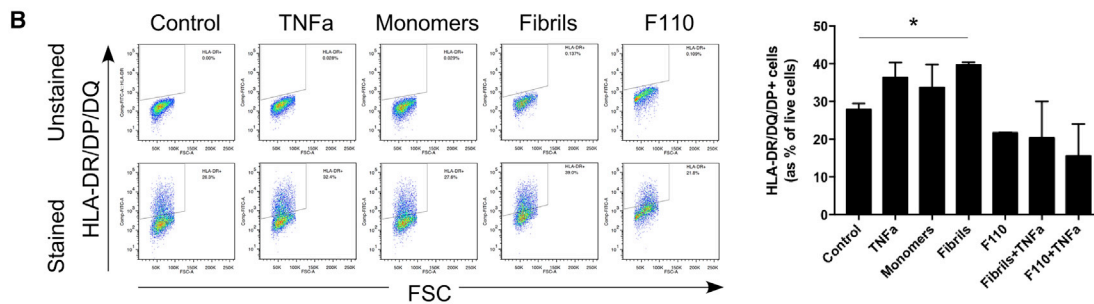
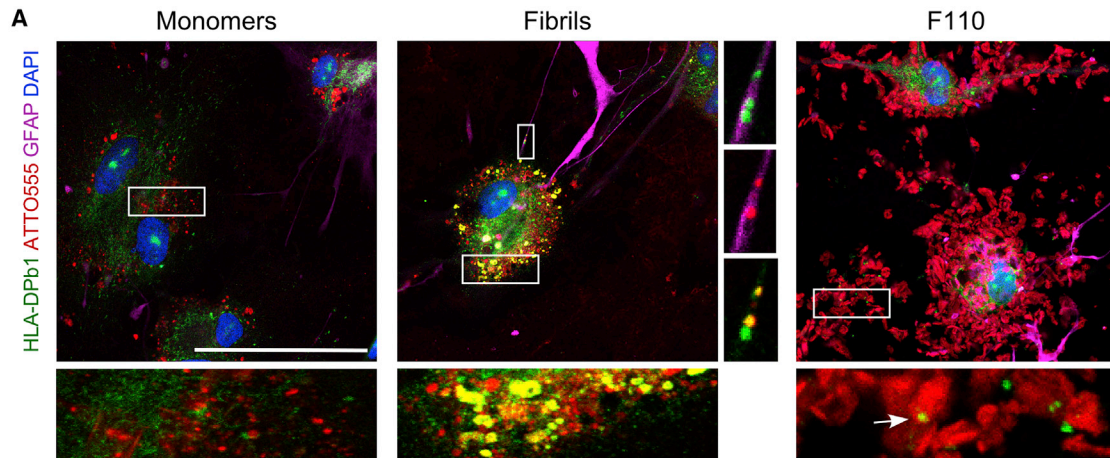
TNF- α (100 ng/ml), and microarray analysis showed up to 100-fold upregulated expression of pro-inflammatory genes compared to control PBS-treated cultures (Table S1; Figure S2). KEGG pathway enrichment analysis revealed activation of TNF- α , nuclear factor kappa-light-chain-enhancer of activated B cells (nuclear factor κ B [NF- κ B]), and chemokine signaling pathways—all associated with inflammation (Hsiao et al., 2013). Nuclear translocation of NF- κ B and release of pro-inflammatory cytokines (interferon γ [IFN- γ], interleukin-1 β [IL-1 β], IL-2, IL-4, IL-6, IL-8, IL-10, IL-12p70, and IL-13) in the growth media (Meeuwssen et al., 2003) were confirmed by immunocytochemistry and quantified using a sensitive multiplex immunoassay (Figure S2), respectively.

We next examined whether the astrocytes would become immune reactive pro-inflammatory when exposed to α SYN monomers, oligomers, or different high-MW α SYN fibrillar polymorphs (ribbons; fibrils; and fibril 65 [F65], fibril 91 [F91], and fibril 110 [F110] polymorphs; Figure S3). We used immunocytochemistry to confirm internalization and aggregation of ATTO488-labeled α SYN species (Figure 1D). To our surprise, human astrocytes treated with the different α SYN species did not exhibit nuclear translocation of NF- κ B (Figure S4). We therefore assessed the presence of pro-inflammatory cytokines as well as TNF- α in the growth media. We did not discover significant increases in cytokine secretion despite the presence of α SYN-positive aggregates in the astrocytes. The total quantity of cytokines secreted was similar between the different α SYN species treatments and similar to PBS-treated control when compared to TNF- α treated cultures (Figure 1E). To rule out the possibility that the astrocytes had responded earlier or that they lacked the ability to respond, we also examined NF- κ B nuclear translocation in human embryonic-stem-cell-derived astrocytes, in a time course study at 1 h, 24 h, and 6 days post-exposure, but found no increase in cytokine secretion (Figure S5).

To further investigate cellular changes triggered by α SYN species in astrocytes, we used microarray analysis and focused on cultures treated with α SYN fibrils and high-MW F110 because these two species resulted in the formation of large cytoplasmic aggregates (Figure 1F). F110 results from a truncated form of α SYN, which is devoid of the 30 C-terminal acidic amino acids

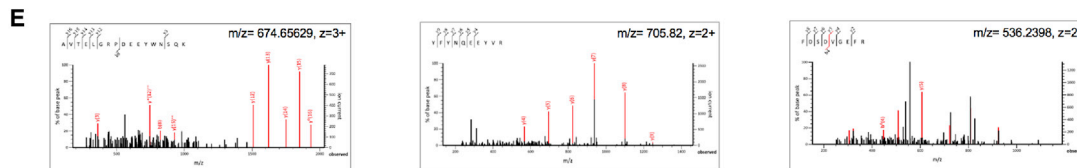
Figure 1. Healthy iPSC-derived astrocytes secrete minimal pro-inflammatory cytokines but upregulate MHC class II genes in response to α SYN treatment

- (A) Differentiation protocol for generating 100-day-old human astrocytes from iPSCs.
 (B) Quantification of astrocytic markers in 100-day-old cultures generated for control iPSC line CSC-37R. Data are mean \pm SEM; n = 5.
 (C) Representative immunostaining for canonical astrocytic markers at day 100. Scale bar, 100 μ m.
 (D) Representative confocal images for α SYN-ATTO-488- and GFAP-stained cultures treated with PBS (control), TNF- α , or various α SYN species. Scale bar, 100 μ m.
 (E) Average total cytokine production (pg/ μ g protein) following treatment of healthy astrocytes, with individual cytokines displayed as percentage of total production. Data are an average of n = 17 for control (control), n = 8 for monomer-treated group, n = 7 for oligomer-treated group, n = 5 for ribbon-treated group, n = 6 for fibril-treated group, n = 6 for F65-treated group, n = 7 for F91-treated group, and n = 12 for the F110-treated group.
 (F) Quantification of the size of the α SYN-ATTO-488-positive inclusions/aggregates present in healthy astrocytes after 6 days of treatment. Each dot represents the length of the aggregate measured. n = 75 aggregates per condition; one-way ANOVA with a Dunnett's multiple comparison test; ****p \leq 0.0001.
 (G) KEGG pathway enrichment analysis shows 10 significantly affected pathways following F110 treatment in healthy astrocytes compared to control. Nine out of 10 pathways contained MHC-class-II-related genes.
 (H) Diagram for genes significantly upregulated, in order of fold-change, following F110 treatment of healthy astrocytes compared to control.
 (I) qRT-PCR analysis of astrocytes treated with TNF- α , α SYN monomers, α SYN fibrils, α SYN F110, α SYN fibrils and TNF- α , or α SYN F110 and TNF- α for 6 days. Data are mean \pm SEM; n = 8 independent experiments per condition. A one-way ANOVA with a Tukey multiple comparison test was used to test the significance for gene fold change in (1) no treatment versus treatment groups (denoted with black line), (2) TNF- α single treatment versus co-treatments (denoted with red line), and (3) α SYN polymorphs single treatment versus co-treatment (denoted with blue line); *p \leq 0.05, **p \leq 0.01, ***p \leq 0.001, ****p \leq 0.0001.



D

Protein family	Accession	Mascot protein score	Mass	Number of MS/MS identifications	Number of identified peptides	Number of unique peptides	Protein description	Species	Gene name	
	258	P01889	113	40777	3	2	2	HLA class I histocompatibility antigen, B-7 alpha chain	Homo sapiens	HLA-B
	226	P04233	129	33950	2	1	1	HLA class II histocompatibility antigen, gamma chain	Homo sapiens	CD74
	458	P20039	66	30483	4	3	3	HLA class II histocompatibility antigen, DRB1-11 beta chain	Homo sapiens	HLA-DRB1



F 13% Sequence protein coverage

```

1  MVCLRLPGGS  CMAVLVTVM  VLSSPLALAG  DTRPRFLEYS  TSECHFNGT
51  ERVRFLDRYF  YNQEYVRFD  SDVGEFRAVT  ELGRPDDEYW  NSQKDFLEDR
101  RAAVDTYCRH  NYGVGESPTV  QRRVHPKIV  YPKTQPLQH  HNLVCSVSG
151  FYPGSIERW  FRNQEKGK  VVSTGLHNG  DWTQQLVML  ETVPRSGEYV
201  TCQVEHPSVT  SPLTVEWRK  SESAQSKMLS  VGGVFLGLL  FLGAGLFYIF
251  RNQKGHSLQ  PRGFLS
    
```

G

List of identified peptides

Sequence	Peptide	Observed m/z	M(expt)	M(calc)	ppm	Ion Score
59-68	R.YFYNQEEYVRF	705.8200	1409.6255	1409.6252	0.22	36
69-77	R.FDSVGEFRA	536.2398	1070.4651	1070.4669	-1.72	31
69-77	R.FDSVGEFRA	536.2422	1070.4696	1070.4669	2.69	20
78-94	RAVTELRGPDDEYNSQK	674.6563	2020.9470	2020.9490	-0.97	21

(legend on next page)

(α SYN 1–110) that can bundle very rapidly prior to and after internalization to cells (Figures 1D and S3). Hardly any genes were upregulated more than 4-fold (Tables S1 and S2). Even after applying a lower 1.5-fold threshold, we found no upregulated genes encoding pro-inflammatory cytokines or chemokines (data not shown; Tables S1 and S2). Interestingly, KEGG enrichment analysis of F110-treated astrocytes did identify pathways associated with major histocompatibility complex (MHC) proteins (Figure 1G). They included human leukocyte antigen (HLA) genes encoding MHC class II proteins, which were significantly upregulated following astrocytic exposure to fibrils and in particular F110 (Figure 1H; Tables S1 and S2).

We used qRT-PCR to confirm the microarray findings and found highly significant altered expression of *HLA-F*, *HLA-DR β 1*, *HLA-DP β 1*, and *HLA-DMA* following the different treatments (Figure 1I). qRT-PCR also confirmed the lack of *CXCL8* gene upregulation following treatment of the astrocytes with α SYN species. Interestingly, co-treatment of the astrocytes with TNF- α and α SYN fibrils or TNF- α and F110 altered the astrocytic expression of *HLA-F*, *HLA-DR β 1*, *HLA-DP β 1*, *CXCL8*, and *HLA-DMA* genes, suggesting that astrocytes had difficulties exhibiting both an immune reactive pro-inflammatory phenotype and an immune reactive antigen-presenting phenotype.

α SYN fibril peptides interact with MHC proteins in human astrocytes, and α SYN fibrils, but not F110, induce relocation of MHC molecules to the astrocytes surface

The discovery of upregulated HLA genes led us to hypothesize that α SYN fibrils and F110 have antigenic properties in astrocytes. Indeed, we observed that the HLA-DP β 1 staining strongly overlapped with α SYN fibrils (Figure 2A, middle panel), but not with α SYN monomers. This finding suggests that from their entry, and during their accumulation in the astrocytes, most α SYN fibrils were degraded to peptides for antigen presentation. Interestingly, only a few HLA-DP β 1/ α SYN F110-positive puncta were observed. However, HLA-DP β 1 was prominently found surrounding the large F110 bundles (Figure 2A, right panel). We speculate that this may be due to the size of F110 bundles and their resistance to proteolytic degradation in astrocytes.

Next, we examined cell surface membrane relocation of MHC class molecules for human astrocytes treated with PBS (control),

TNF- α , α SYN monomers, α SYN fibrils, or F110. Interestingly, fluorescence-activated cell sorting (FACS) analysis showed a significant increase in the percentage of MHC-class-II-positive astrocytes in cultures exposed to α SYN fibrils but not in cultures exposed to F110 (Figure 2B). No significant change was identified at the earlier time point (1 day post-treatment; data not shown) despite significantly increased *HLA-DP β 1* gene expression seen 1 day post-treatment (Figure S6). These data indicate that astrocytes had difficulties in degrading the fibrils for presentation by MHC class II molecules and/or that they may have engaged into cross presentation by MHC class I molecules. As limited proteolysis of fibrils has been previously described (Loria et al., 2017; Pieri et al., 2016a), we examined cross presentation. α SYN fibril treatment caused a massive increase in HLA-F-positive astrocytes, despite unchanged mRNA levels (Figures 1I and 2C). These data indicate a relocation of existing HLA-F molecules to the cell surface in astrocytes, either for presentation of α SYN fibril peptides or for open conformer presentation (Dulberger et al., 2017). Interestingly, the increase in *HLA-F* transcripts, mediated by TNF- α treatment, did not translate into increased HLA-F molecules at the astrocyte surface membrane. Additionally, co-treatment of astrocytes with both TNF- α and fibrils antagonized the effect of the fibrils alone on relocation of MHC molecules to the astrocyte cell surface (Figures 2B, 2C, and S6).

To establish whether α SYN fibrils and MHC molecules interact, we treated astrocytes with biotin-labeled α SYN fibrils, prepared membrane fractions, pulled down the fibrils, and identified the associated proteins by using a proteomics approach. Western blot analysis showed the presence of HLA-DP β 1 immuno-reactive bands of different MWs in the membrane fraction in astrocytes treated with the biotinylated α SYN fibrils only. To further demonstrate the MHC protein interaction with α SYN fibrils and to determine which MHC haplotypes interact with α SYN fibrils, we subjected the pulled down astrocyte membrane proteins to trypsin digestion and identified the resulting peptides by nano-LC MS/MS (liquid chromatography-tandem mass spectrometry; Figure S6). Control samples were prepared from astrocytes not exposed to α SYN fibrils as previously described (Shrivastava et al., 2019). We identified 1,020 protein families with at least 1 peptide (mascot ion score of >15) in the membrane

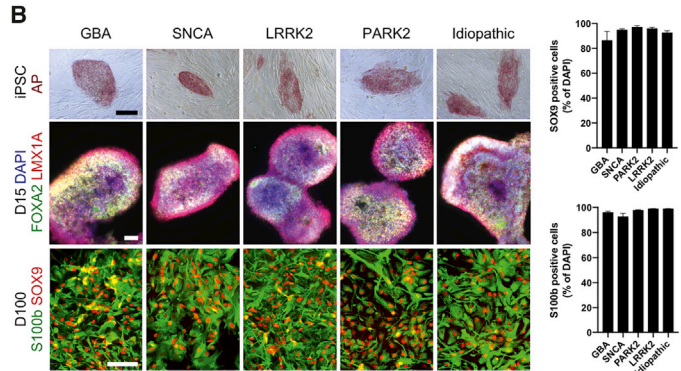
Figure 2. α SYN-fibril-treated healthy astrocytes acquire an antigen-presenting phenotype and fibril peptides physical interaction with MHC class molecules

- (A) Representative confocal images for astrocyte cultures stained for α SYN-ATTO555, HLA-DP β 1, GFAP, and DAPI, following their exposure to monomers, fibrils, or F110. Extensive colocalization follows fibril treatment only. Scale bar, 100 μ m.
- (B) Flow cytometry analysis and quantification of HLA-DR/DP/DQ-positive healthy astrocytes treated with either PBS (control), 100 ng/ml TNF- α , or 10 μ M α SYN (monomers, fibrils, or F110) for 6 days. Because the treatments changed the morphology of the cells, the percentages of positive cells were calculated using gating for non-stained cells. Data are mean \pm SEM; n = 2 independent experiments per condition; t test; *p \leq 0.05.
- (C) Flow cytometry analysis and quantification of HLA-F-positive healthy astrocytes treated with either PBS (control), 100 ng/ml TNF- α , or 10 μ M α SYN (monomers, fibrils, or F110) for 6 days. Because the treatments changed the morphology of the cells, the percentages of positive cells were calculated using gating for non-stained cells. Data are mean \pm SEM; n = 2 independent experiments per condition; t test; *p \leq 0.05.
- (D) A total of 1,020 and 126 protein families were identified with at least 1 peptide (Mascot ions core \geq 15) from pull-downs performed on membrane fractions from cells exposed or not to biotinylated α SYN fibrils, respectively. Three MHC protein members were identified in astrocytes exposed to biotinylated α SYN fibrils; two were identified in the MHC class II family. No MHC proteins were detected in untreated astrocytes.
- (E) The MS/MS fragmentation spectra of three HLA-DR β 1 (P20039) tryptic peptides identified after pull-down of biotinylated α SYN fibrils. Spectra show primary structure, mascot ion score, m/z, and mass accuracy of the fragmented precursor peptide. The primary structure was determined from the y (red) fragment ions.
- (F) Primary structure coverage of HLA class II histocompatibility antigen DR β 1-11 beta chain (HLA-DR β 1). The 13% sequence coverage of HLA-DR β 1 is marked in red.
- (G) Sequence and properties of the four HLA-DR β 1 tryptic peptides, identified by nano-LC-MS/MS analysis.

A

Clone ID	Diagnosis	Molecular analysis	Gender	Reprogramming	Reference
CSC-10A	PD (GBA)	<i>p.L444P/WT</i>	Female	Sendai virus	2
CSC-10B	PD (GBA)	<i>p.L444P/WT</i>	Female	Sendai virus	2
CSC-10C	PD (GBA)	<i>p.L444P/WT</i>	Female	Sendai virus	2
CSC-7A	PD (PARK2)	<i>p.C273W/p.C273W</i>	Female	Retrovirus	2
CSC-7B	PD (PARK2)	<i>p.C273W/p.C273W</i>	Female	Retrovirus	2
CSC-21B	PD (PARK2)	<i>p.A275W/p.A275W</i>	Female	Sendai virus	2
CSC-18A	PD (LRRK2)	<i>p.R1441C/WT</i>	Male	Sendai virus	2
CSC-19A	PD (LRRK2)	<i>p.G2019S/WT</i>	Male	Sendai virus	2
CSC-3G	PD (SNCA)	triplication	Female	Retrovirus	1; 2
CSC-3S	PD (SNCA)	triplication	Female	Retrovirus	1; 2
CSC-28N #	PD (SNCA)	triplication	Female	Sendai virus	this study
CSC-26B	Idiopathic PD		Female	Sendai virus	this study
CSC-27A	Idiopathic PD		Male	Sendai virus	this study
CSC-27K	Idiopathic PD		Male	Sendai virus	this study

CSC-28N and CSC-3G and -3S are from the same patient, but differently reprogrammed

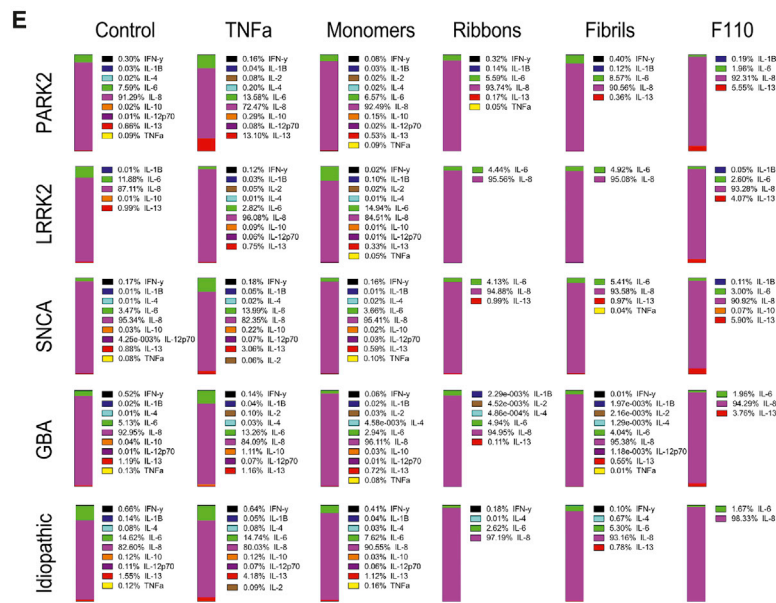
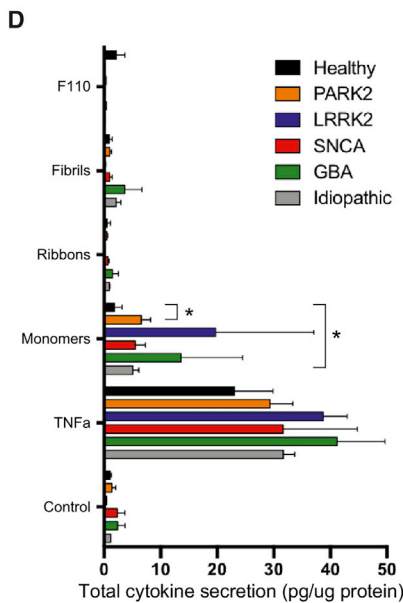
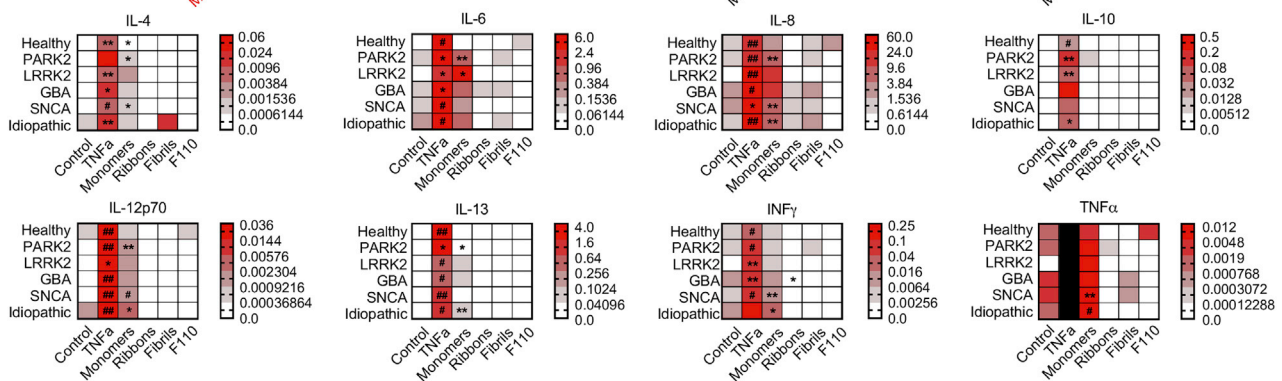


C

Genotype	IL-1β	IL-2	IL-4	IL-6	IL-8	IL-10	IL-12p70	IL-13	INFγ	TNFα
Healthy	17	7	8	5	6	12	2	2	2	2
PARK2	10	6	5	5	6	1	3	3	3	3
LRRK2	5	4	4	2	4	1	2	2	2	2
GBA	9	7	7	6	7	1	3	3	3	3
SNCA	8	5	5	5	6	1	3	3	3	3
Idiopathic	7	5	5	5	5	1	3	3	3	3

Note: numbers in squares represent number of samples analyzed per condition from 2-4 differentiations per clone.

* = P ≤ 0.05
** = P ≤ 0.01
= P ≤ 0.0001
= P ≤ 0.001
N/A



(legend on next page)

fraction (Figures 2D and 2E; Table S3). The HLA class II histocompatibility antigen DR β 1-11 beta chain was identified with a high degree of certainty, confirming the interaction between α SYN fibril peptides and MHC molecules (Figures 2F and 2G).

PD-variant-containing astrocytes display increased production of pro-inflammatory cytokines when exposed to α SYN monomers but not when exposed to α SYN fibrils or F110

A recent study suggested that PD astrocytes may show an exacerbated response to pro-inflammatory stressors (Sonninen et al., 2020). We therefore assessed pro-inflammatory cytokine release from astrocytes differentiated from iPSCs generated from PD patients with genetic variants in *PARK2*, *LRRK2*, *SNCA*, or *GBA*, as well as from patients with idiopathic PD (Figure 3A).

First, we generated iPSCs from the PD variants and idiopathic PD fibroblasts and then differentiated them to astrocytes. By day 15, the neural progenitors acquired a ventral midbrain identity, as confirmed by immunocytochemistry for LMX1A and FOXA2 markers (Figure 3B). By day 100, the cultures were enriched in astrocytes immuno-positive for S100 β and SOX9 (Figure 3B). Astrocytes treated with TNF- α released high amounts of pro-inflammatory cytokines, measured using a sensitive multiplex immunoassay (Figure 3C), and relocated NF- κ B to the nucleus (Figure S4). PD astrocytes exposed to high MW α SYN species released low total levels of pro-inflammatory cytokines, ranging from 0.44 to 2.39 pg/ μ g (Figure 3D). However, we found at least a 2-fold increase in secretion of the main pro-inflammatory cytokines IL-6 and IL-8 in PD astrocytes compared to control healthy astrocytes upon exposure to α SYN monomers (Figure 3D). Astrocytes with the *PARK2*-variant background exhibited highly significant changes in pro-inflammatory cytokine production (Figures 3D and 3E).

High-MW α SYN species impair ATP-generating mitochondrial respiration in healthy and in *PARK2*-variant PD astrocytes

Recent evidence suggests altered mitochondrial fusion and fragmentation rates following exposure to α SYN fibrils and on-fibrillar assembly pathway oligomers in human neurons and astrocytes derived from pluripotent stem cells (Gribaudo et al., 2019; Rostami et al., 2017). Therefore, we investigated whether the astrocytic exposure to α SYN monomers, fibrils, or F110

would impair mitochondrial function. Untreated cultures, following normalization to citrate synthase activity, had no significant difference in basal, uncoupled, or coupled (ATP generating) respiration in astrocytes when using Seahorse analysis (data not shown). Similar results were obtained when cultures were normalized to the total amount of protein (data not shown). Control (non-PD) astrocytes exposed to α SYN fibrils, but not α SYN monomers or F110, had a significant decrease in basal, uncoupled, and coupled mitochondrial respiration (Figure 4A). Interestingly, *PARK2*-variant PD astrocytes, which showed the most significant change in release of pro-inflammatory cytokines following exposure to α SYN monomers, exhibited a more pronounced decrease in basal, uncoupled, and coupled respiration upon exposure to α SYN fibrils or F110 polymorphs than healthy astrocytes (Figure 4B). Citrate synthase activity was not significantly changed in control and *PARK2*-variant PD astrocytes following addition of α SYN species (data not shown). Interestingly, the exposure of *PARK2*-variant PD astrocytes to α SYN fibrillar polymorphs mirrored the deleterious effect on mitochondrial function of the *PARK2*-variant PD astrocyte exposed to TNF- α (Figures 4C and 4D).

DISCUSSION

The specificity of the astrocyte immune reactive responses in PD is poorly understood. For example, it is still unclear if various well-defined species of α SYN that may form in the PD brain can influence the cellular behavior of astrocytes. To investigate astrocyte immune reactivity in PD, we first exposed non-PD human iPSC-derived astrocytes to α SYN assemblies with *in vitro* and *in vivo* seeding propensity (Bousset et al., 2013; Peelaerts et al., 2015). All the tested cytokines showed an elevated response to TNF- α treatment, but there was no increase in cytokine production following exposure to the α SYN species. However, α SYN fibrillar polymorphs triggered changes in the expression of HLA genes encoding MHC class I and II proteins. Moreover, we found the astrocytic immune reactive pro-inflammatory and antigen-presenting phenotypes triggered by TNF- α and α SYN fibrils, respectively, coupled to impaired ATP-generating mitochondrial respiration.

Astrocytic expression of MHC class I and II gene products has been previously reported, and MHC-class-II-positive astrocytes were identified at the edge of lesions in multiple sclerosis brain

Figure 3. PD astrocytes show functional differences and are prone to release cytokines when treated with monomeric α SYN

(A) Overview of PD iPSC lines and clones used in this study (1, Holmqvist et al., 2016; 2, Djelloul et al., 2015).

(B) Representative images of alkaline phosphatase (AP)-positive iPSCs used to generate FOXA2 and LMX1A double-positive midbrain progenitors differentiated into S100 β and SOX9 double-positive astrocytes. Quantification of S100 β - and SOX9-positive astrocytes aged 100 days is shown in graphs in the right panels; data are mean \pm SEM; n = 5 or 6 for each variant. Scale bar, 100 μ m.

(C) Summary heatmaps of pro-inflammatory cytokine secretion, normalized using total protein (pg/ μ g protein), in healthy, *PARK2*, *LRRK2*, *GBA*, *SNCA*, and idiopathic astrocytes following no treatment (NT) or treatment with TNF- α , monomers, ribbons, fibrils, or F110. NT and TNF- α -treated astrocytes were analyzed separately by using unpaired two-tailed Student's t tests; NT and monomer-, ribbon-, and fibril-treated groups were compared using a one-way ANOVA with a Dunnett's multiple comparison test; F110 and remaining forms of α SYN assemblies (not shown) were compared separately using one-way ANOVA with a Dunnett's multiple comparison test; n is shown in (C) and is from 2–3 independent clones with 2–4 differentiations per clone; *p \leq 0.05; **p \leq 0.01, #p \leq 0.001, ##p \leq 0.0001.

(D) Average total pro-inflammatory cytokine production (pg/ μ g protein) from PD astrocytes following different treatments. Data are mean \pm SEM; n = 3 experiments for 2 to 3 clones used per variant. For each treatment, the variants were compared using a one-way ANOVA with a Dunnett's multiple comparison test; *PARK2*-variant and idiopathic PD astrocytes showed p \leq 0.05 (*) when compared to non-PD astrocytes (healthy).

(E) Percentage of total cytokine production following various treatments in PD astrocytes.

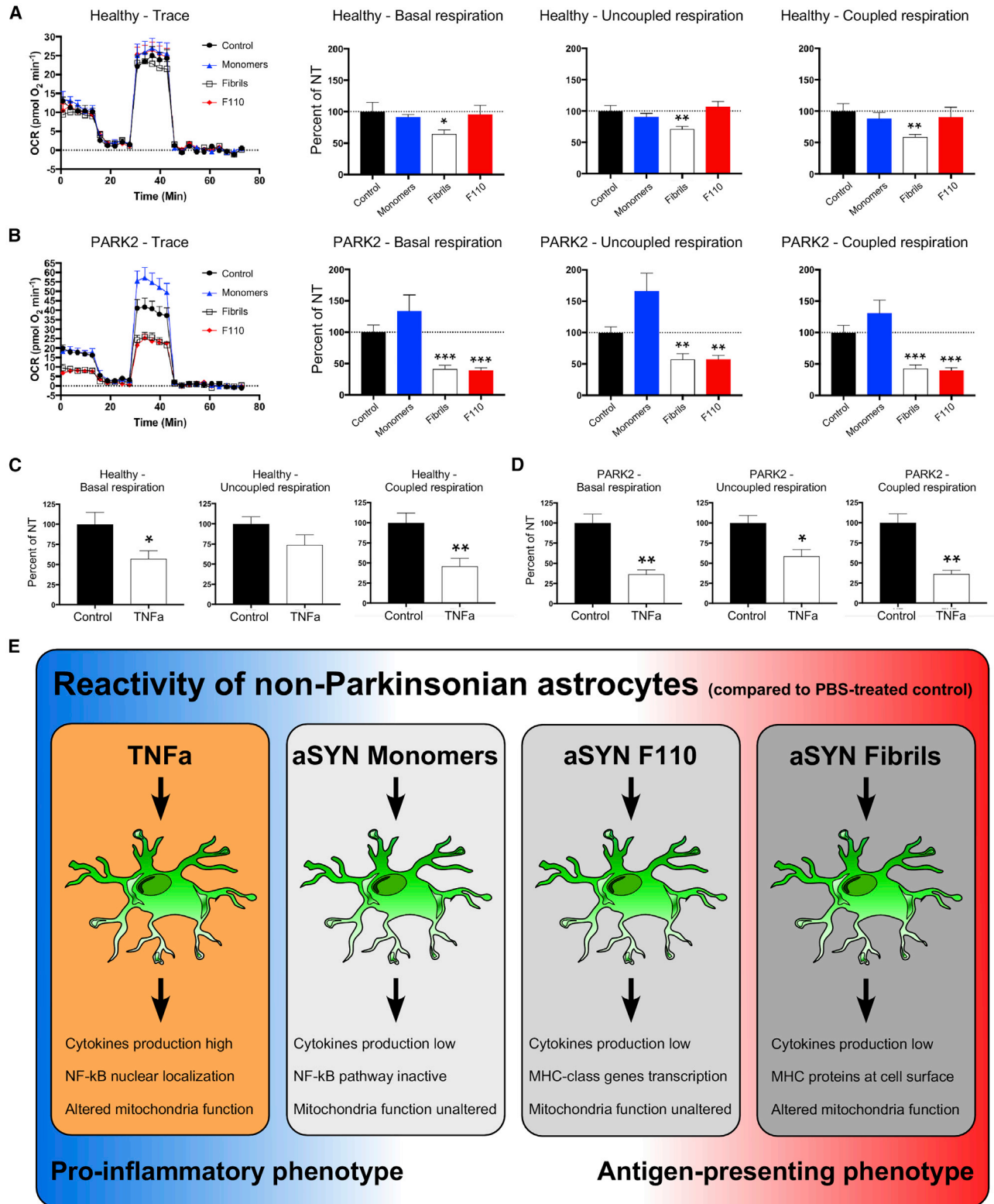


Figure 4. Mitochondrial respiration impairment in PARK2 variants following α SYN treatment

(A) Seahorse analysis of mitochondrial respiration following treatment with monomers, fibrils, or F110 in healthy astrocytes showed a significant decrease in uncoupled and coupled citrate-synthase-normalized respiration (depicted as % of NT cells).

(legend continued on next page)

tissue (Ransohoff and Estes, 1991; Vardjan et al., 2012). Moreover, astrocytes were shown to phagocytose large neuronal NeuN-positive debris after brain ischemia (Morizawa et al., 2017). Here, we confirmed internalization of fibrillar α SYN polymorphs, which increase expression of an HLA-DMA gene that encodes for the enzyme that facilitate CLIP (class II-associated invariant chain peptide) removal from the MHC class II molecules, allowing them to interact with antigen peptides (Roche and Furuta, 2015), and importantly direct interaction between α SYN fibril peptides and MHC class II proteins in pull-down experiments. Although both fibrils and F110 triggered increased MHC class II gene expression, overlap between MHC class II protein HLA-DP β 1 and α SYN appeared mainly in astrocytes treated with α SYN fibrils. In contrast, HLA-DP β 1 staining was prominent surrounding the large F110 aggregates that had formed prior to being phagocytosed. These data may suggest that temporally accumulated α SYN fibrils in astrocytes were progressively degraded into peptides that bound MHC class II proteins. This was not possible for larger F110 fibril polymorphs that had been phagocytosed. Surprisingly, astrocytes containing α SYN fibrils, overlapping with HLA-DP β 1, almost exclusively relocated MHC class I HLA-F molecules at the astrocyte surface. These data suggested that the astrocytes had adopted an antigen-presenting phenotype, either by cross presentation of α SYN peptides or empty open conformer presentation (Dulberger et al., 2017), similar to oligodendrocytes in a model for multiple sclerosis (Harrington et al., 2020; Kirby et al., 2019). Interestingly, co-treatment of astrocytes with both TNF- α and α SYN fibrils significantly lowered the effect provided by TNF- α or α SYN fibrillar polymorphs alone. Altogether, these data are extremely important as they could imply that the astrocytes' anti- α SYN response could be altered in the presence of pro-inflammatory cytokines and diminished by large aggregates or degradation-resistant fibrils, potentially explaining the permanent increase in α SYN aggregation during disease progression.

α SYN-positive inclusions have been reported in astrocytes from PD post-mortem brains (Braak et al., 2007; Wakabayashi et al., 2000). Moreover, evidence suggests that prolonged astrocytic dysfunction and reactive toxic astrocytes might contribute to the demise of neurons (Kuter et al., 2018; Liddel et al., 2017). According to our data, healthy astrocytes seem to be able to manage the additional burden of various α SYN species by showing lower total secretion of pro-inflammatory cytokines for most α SYN species. However, the cellular metabolism was altered. Mitochondrial respiration declined in α SYN and TNF- α -treated control astrocytes. This decline was exacerbated in *PARK2*-variant PD astrocytes. These important functional consequences of α SYN fibrils and TNF- α burden might ultimately impact the survival of the neurons, in particular dopaminergic neurons in PD, by diminishing the supportive capacity of the astrocytes. It will be important to further compare the metabolic al-

terations displayed by astrocytes carrying different variations (e.g., *GBA1* versus *PINK* versus *PARK2*, and other variants).

Our findings highlight various responses of astrocytes to TNF- α and α SYN species and provide insights into the immune reactive role of astrocytes in neurodegeneration. This knowledge could help develop therapeutic approaches to delay the progression of PD and other synucleinopathies.

STAR★METHODS

Detailed methods are provided in the online version of this paper and include the following:

- KEY RESOURCES TABLE
- RESOURCE AVAILABILITY
 - Lead contact
 - Materials availability
 - Data and code availability
- EXPERIMENTAL MODEL AND SUBJECT DETAILS
 - Ethics
 - iPSC line derivation and production of astrocytes
- METHOD DETAILS
 - iPSC generation
 - Differentiation of iPSCs to astrocytes
 - α SYN purification and species preparation
 - Gene expression analysis
 - Flow cytometry analysis
 - Quantitative RT-PCR
 - Pro-inflammatory cytokine analysis
 - Immunocytochemical analysis
 - Pull-down assay and mass spectrometry
 - Seahorse analysis
- QUANTIFICATION AND STATISTICAL ANALYSIS
 - Statistics
 - Aggregate size counting
 - Bioinformatics

SUPPLEMENTAL INFORMATION

Supplemental information can be found online at <https://doi.org/10.1016/j.celrep.2021.108895>.

ACKNOWLEDGMENTS

We thank AnnaKarin Oldén and Marianne Juhlin for their outstanding technical assistance and the staff at the cytogenetic units at Lund University Hospital for preparing the samples for karyotyping. We are also thankful to the "Cell Line and DNA Biobank from Patients affected by Genetic Diseases" (Istituto G. Gaslini, Genova, Italy) and the "Parkinson Institute Biobank" members of the Telethon Network of Genetic Biobanks funded by Telethon Italy (project no. GTB12001; <http://biobanknetwork.telethon.it>) for providing fibroblast samples. This work was specifically supported by The Michael J. Fox Foundation; the Swedish Parkinson Foundation (Parkinsonfonden); the Holger Crafoord Foundation; the Thelma Zoegas Foundation; the Shaking Generation

(B) In *PARK2*-variant astrocytes treated with monomers, fibrils, or F110 had a significant effect on basal, uncoupled, and coupled citrate-synthase-normalized respiration (depicted as % of NT cells).

(C and D) TNF- α treatment significantly decreased the basal and coupled respiratory capacity in healthy and *PARK2*-variant astrocytes.

(E) Graphical summary of the overall effects of the various treatments on healthy astrocytes. Seahorse data are mean \pm SEM; a t test was used to compare the groups to control; * $p \leq 0.05$; ** $p \leq 0.01$, # $p \leq 0.001$, ## $p \leq 0.0001$. $n = 6-8$ technical replicates of 2 biological replicates.

Foundation; the Åke Wibergs Foundation; the Magnus Bergvall's Foundation; the Greta och Johan Kocks Foundation; donations for science, medicine, and technology at Fysiografen in Lund; the Swedish Research Council (grant VR-2015-03684 to L.R.); Brainstem - Stem Cell Center for Excellence in Neurology funded by the Innovation Fund Denmark; and the Olav Thon Foundation in Norway to L.R. The M.V. lab is supported by the Swedish Research Council (grant VR-2015-02510). The R.M. lab was supported by grants from the EC Joint Programme on Neurodegenerative Diseases (JPND-NeuTARGETs-ANR-14-JPCD-0002-02 and JPND-SYNACTION-ANR-15-JPWG-0012-03), the Centre National de la Recherche Scientifique, The Fondation pour la Recherche Médicale (contract DEQ 20160334896), a "Coup d'Élan a la Recherche Francaise" award from Fondation Bettencourt Schueller, the Fondation Simone et Cino Del Duca of the Institut de France, and the European Union (EU/EFPIA/Innovative Medicine Initiative 2 Joint Undertaking IMPRIND grant agreement no 116060; <https://www.imprind.org>). The L.R. lab is supported by the Strong Research Environment MultiPark at Lund University and the EC Joint Programme on Neurodegenerative Diseases (JPND-MADGIC-VR-2015-06798).

AUTHOR CONTRIBUTIONS

K.R. designed the study, performed experiments, analyzed data, and wrote the manuscript. G.T. analyzed Affymetrix data. L.B. generated and characterized all biochemically and structurally α SYN forms. S.P. assisted with Seahorse experiments and data analysis. V.R. performed the mass spectrometry experiment and supervised the pull-down assay. E.S. improved the protocol for generating astrocytes. Y.P. performed generation and characterization of iPSCs. J.S. performed the pull-down assay. T.C.S. performed and analyzed qRT-PCR. C.A. assisted with FACS and α SYN treatment. A.C. performed generation of karyograms and supervision of analysis. S.G. was responsible for provision of study material. K.F. performed data analysis and interpretation. E.E. performed data analysis and interpretation. M.V. performed data analysis and interpretation and editing of the manuscript. R.M. contributed to study design, analysis of data, and editing of the manuscript. L.R. designed study, assisted with generation and characterization of iPSCs, analyzed data, and wrote manuscript. All authors gave input on the manuscript and approved its content.

DECLARATION OF INTERESTS

The authors declare no competing interests

Received: February 8, 2019

Revised: December 23, 2021

Accepted: March 2, 2021

Published: March 23, 2021

REFERENCES

Booth, H.D.E., Hirst, W.D., and Wade-Martins, R. (2017). The Role of Astrocyte Dysfunction in Parkinson's Disease Pathogenesis. *Trends Neurosci.* **40**, 358–370.

Bousset, L., Pieri, L., Ruiz-Arlandis, G., Gath, J., Jensen, P.H., Habenstein, B., Madiona, K., Olieric, V., Böckmann, A., Meier, B.H., and Melki, R. (2013). Structural and functional characterization of two alpha-synuclein strains. *Nat. Commun.* **4**, 2575.

Braak, H., Sastre, M., and Del Tredici, K. (2007). Development of alpha-synuclein immunoreactive astrocytes in the forebrain parallels stages of intraneuronal pathology in sporadic Parkinson's disease. *Acta Neuropathol.* **114**, 231–241.

Djelloul, M., Holmqvist, S., Boza-Serrano, A., Azevedo, C., Yeung, M.S., Goldwurm, S., Frisén, J., Deierborg, T., and Roybon, L. (2015). Alpha-Synuclein Expression in the Oligodendrocyte Lineage: an In Vitro and In Vivo Study Using Rodent and Human Models. *Stem Cell Reports* **5**, 174–184.

Dulberger, C.L., McMurtrey, C.P., Hölzemer, A., Neu, K.E., Liu, V., Steinbach, A.M., Garcia-Beltran, W.F., Sulak, M., Jabri, B., Lynch, V.J., et al. (2017). Hu-

man Leukocyte Antigen F Presents Peptides and Regulates Immunity through Interactions with NK Cell Receptors. *Immunity* **46**, 1018–1029.e7.

Gentleman, R.C., Carey, V.J., Bates, D.M., Bolstad, B., Dettling, M., Dudoit, S., Ellis, B., Gautier, L., Ge, Y., Gentry, J., et al. (2004). Bioconductor: open software development for computational biology and bioinformatics. *Genome Biol.* **5**, R80.

Ghee, M., Melki, R., Michot, N., and Mallet, J. (2005). PA700, the regulatory complex of the 26S proteasome, interferes with alpha-synuclein assembly. *FEBS J.* **272**, 4023–4033.

Griboaud, S., Tixador, P., Bousset, L., Fenyi, A., Lino, P., Melki, R., Peyrin, J.M., and Perrier, A.L. (2019). Propagation of α -Synuclein Strains within Human Reconstructed Neuronal Network. *Stem Cell Reports* **12**, 230–244.

Gu, Z., Eils, R., and Schlesner, M. (2016). Complex heatmaps reveal patterns and correlations in multidimensional genomic data. *Bioinformatics* **32**, 2847–2849.

Guerrero-Ferreira, R., Taylor, N.M., Arteni, A.A., Kumari, P., Mona, D., Ringler, P., Britschgi, M., Lauer, M.E., Makky, A., Verasdonck, J., et al. (2019). Two new polymorphic structures of human full-length alpha-synuclein fibrils solved by cryo-electron microscopy. *eLife* **8**, e48907.

Harrington, E.P., Bergles, D.E., and Calabresi, P.A. (2020). Immune cell modulation of oligodendrocyte lineage cells. *Neurosci. Lett.* **715**, 134601.

Holmqvist, S., Brouwer, M., Djelloul, M., Diaz, A.G., Devine, M.J., Hammarberg, A., Fog, K., Kunath, T., and Roybon, L. (2015). Generation of human pluripotent stem cell reporter lines for the isolation of and reporting on astrocytes generated from ventral midbrain and ventral spinal cord neural progenitors. *Stem Cell Res. (Amst.)* **15**, 203–220.

Holmqvist, S., Lehtonen, S., Chumarina, M., Puttonen, K.A., Azevedo, C., Lebdeeva, O., Ruponen, M., Oksanen, M., Djelloul, M., Collin, A., et al. (2016). Creation of a library of induced pluripotent stem cells from Parkinsonian patients. *NPJ Parkinsons Dis.* **2**, 16009.

Hsiao, H.Y., Chen, Y.C., Chen, H.M., Tu, P.H., and Chern, Y. (2013). A critical role of astrocyte-mediated nuclear factor- κ B-dependent inflammation in Huntington's disease. *Hum. Mol. Genet.* **22**, 1826–1842.

Kirby, L., Jin, J., Cardona, J.G., Smith, M.D., Martin, K.A., Wang, J., Strasburger, H., Herbst, L., Alexis, M., Karnell, J., et al. (2019). Oligodendrocyte precursor cells present antigen and are cytotoxic targets in inflammatory demyelination. *Nat. Commun.* **10**, 3887.

Kuter, K., Olech, Ł., and Glowacka, U. (2018). Prolonged Dysfunction of Astrocytes and Activation of Microglia Accelerate Degeneration of Dopaminergic Neurons in the Rat Substantia Nigra and Block Compensation of Early Motor Dysfunction Induced by 6-OHDA. *Mol. Neurobiol.* **55**, 3049–3066.

Lee, H.J., Suk, J.E., Patrick, C., Bae, E.J., Cho, J.H., Rho, S., Hwang, D., Masliah, E., and Lee, S.J. (2010). Direct transfer of alpha-synuclein from neuron to astroglia causes inflammatory responses in synucleinopathies. *J. Biol. Chem.* **285**, 9262–9272.

Li, B., Ge, P., Murray, K.A., Sheth, P., Zhang, M., Nair, G., Sawaya, M.R., Shin, W.S., Boyer, D.R., Ye, S., et al. (2018). Cryo-EM of full-length α -synuclein reveals fibril polymorphs with a common structural kernel. *Nat. Commun.* **9**, 3609.

Liddel, S.A., Guttenplan, K.A., Clarke, L.E., Bennett, F.C., Bohlen, C.J., Schirmer, L., Bennett, M.L., Münch, A.E., Chung, W.S., Peterson, T.C., et al. (2017). Neurotoxic reactive astrocytes are induced by activated microglia. *Nature* **541**, 481–487.

Loria, F., Vargas, J.Y., Bousset, L., Syan, S., Salles, A., Melki, R., and Zurzolo, C. (2017). α -Synuclein transfer between neurons and astrocytes indicates that astrocytes play a role in degradation rather than in spreading. *Acta Neuropathol.* **134**, 789–808.

Makky, A., Bousset, L., Polesel-Maris, J., and Melki, R. (2016). Nanomechanical properties of distinct fibrillar polymorphs of the protein α -synuclein. *Sci. Rep.* **6**, 37970.

Meeuwssen, S., Persoon-Deen, C., Sbsi, M., Ravid, R., and van Noort, J.M. (2003). Cytokine, chemokine and growth factor gene profiling of cultured human astrocytes after exposure to proinflammatory stimuli. *Glia* **43**, 243–253.

- Morizawa, Y.M., Hirayama, Y., Ohno, N., Shibata, S., Shigetomi, E., Sui, Y., Nabekura, J., Sato, K., Okajima, F., Takebayashi, H., et al. (2017). Reactive astrocytes function as phagocytes after brain ischemia via ABCA1-mediated pathway. *Nat. Commun.* **8**, 28.
- Peelaerts, W., Bousset, L., Van der Perren, A., Moskalyuk, A., Pulizzi, R., Giugliano, M., Van den Haute, C., Melki, R., and Baekelandt, V. (2015). α -Synuclein strains cause distinct synucleinopathies after local and systemic administration. *Nature* **522**, 340–344.
- Pekny, M., and Pekna, M. (2016). Reactive gliosis in the pathogenesis of CNS diseases. *Biochim. Biophys. Acta* **1862**, 483–491.
- Pieri, L., Chafey, P., Le Gall, M., Clary, G., Melki, R., and Redeker, V. (2016a). Cellular response of human neuroblastoma cells to α -synuclein fibrils, the main constituent of Lewy bodies. *Biochim. Biophys. Acta* **1860**, 8–19.
- Pieri, L., Madiona, K., and Melki, R. (2016b). Structural and functional properties of prefibrillar α -synuclein oligomers. *Sci. Rep.* **6**, 24526.
- Poewe, W., Seppi, K., Tanner, C.M., Halliday, G.M., Brundin, P., Volkman, J., Schrag, A.E., and Lang, A.E. (2017). Parkinson disease. *Nat. Rev. Dis. Primers* **3**, 17013.
- Pomeshchik, Y., Klementieva, O., Gil, J., Martinsson, I., Hansen, M.G., de Vries, T., Sancho-Balsells, A., Russ, K., Savchenko, E., Collin, A., et al. (2020). Human iPSC-Derived Hippocampal Spheroids: An Innovative Tool for Stratifying Alzheimer Disease Patient-Specific Cellular Phenotypes and Developing Therapies. *Stem Cell Reports* **15**, 256–273.
- Ransohoff, R.M., and Estes, M.L. (1991). Astrocyte expression of major histocompatibility complex gene products in multiple sclerosis brain tissue obtained by stereotactic biopsy. *Arch. Neurol.* **48**, 1244–1246.
- Roche, P.A., and Furuta, K. (2015). The ins and outs of MHC class II-mediated antigen processing and presentation. *Nat. Rev. Immunol.* **15**, 203–216.
- Rostami, J., Holmqvist, S., Lindström, V., Sigvardson, J., Westermark, G.T., Ingelsson, M., Bergström, J., Roybon, L., and Erlandsson, A. (2017). Human Astrocytes Transfer Aggregated Alpha-Synuclein via Tunneling Nanotubes. *J. Neurosci.* **37**, 11835–11853.
- Roybon, L., Lamas, N.J., Garcia, A.D., Yang, E.J., Sattler, R., Lewis, V.J., Kim, Y.A., Kachel, C.A., Rothstein, J.D., Przedborski, S., et al. (2013). Human stem cell-derived spinal cord astrocytes with defined mature or reactive phenotypes. *Cell Rep.* **4**, 1035–1048.
- Shrivastava, A.N., Redeker, V., Pieri, L., Bousset, L., Renner, M., Madiona, K., Mailhes-Hamon, C., Coens, A., Buée, L., Hantraye, P., et al. (2019). Clustering of Tau fibrils impairs the synaptic composition of α 3-Na⁺/K⁺-ATPase and AMPA receptors. *EMBO J.* **38**, e99871.
- Sloan, S.A., Darmanis, S., Huber, N., Khan, T.A., Birey, F., Caneda, C., Reimer, R., Quake, S.R., Barres, B.A., and Pasca, S.P. (2017). Human Astrocyte Maturation Captured in 3D Cerebral Cortical Spheroids Derived from Pluripotent Stem Cells. *Neuron* **95**, 779–790.e6.
- Sonninen, T.M., Hämäläinen, R.H., Koskivi, M., Oksanen, M., Shakirzyanova, A., Wojciechowski, S., Puttonen, K., Naumenko, N., Goldsteins, G., Laham-Karam, N., et al. (2020). Metabolic alterations in Parkinson's disease astrocytes. *Sci. Rep.* **10**, 14474.
- Spillantini, M.G., Schmidt, M.L., Lee, V.M., Trojanowski, J.Q., Jakes, R., and Goedert, M. (1997). Alpha-synuclein in Lewy bodies. *Nature* **388**, 839–840.
- Spillantini, M.G., Crowther, R.A., Jakes, R., Hasegawa, M., and Goedert, M. (1998). alpha-Synuclein in filamentous inclusions of Lewy bodies from Parkinson's disease and dementia with lewy bodies. *Proc. Natl. Acad. Sci. USA* **95**, 6469–6473.
- Sun, Y., Hou, S., Zhao, K., Long, H., Liu, Z., Gao, J., Zhang, Y., Su, X.D., Li, D., and Liu, C. (2020). Cryo-EM structure of full-length α -synuclein amyloid fibril with Parkinson's disease familial A53T mutation. *Cell Res.* **30**, 360–362.
- Vardjan, N., Gabrijel, M., Potokar, M., Svaiger, U., Kreft, M., Jeras, M., de Pablo, Y., Faiz, M., Pekny, M., and Zorec, R. (2012). IFN- γ -induced increase in the mobility of MHC class II compartments in astrocytes depends on intermediate filaments. *J. Neuroinflammation* **9**, 144.
- Wakabayashi, K., Hayashi, S., Yoshimoto, M., Kudo, H., and Takahashi, H. (2000). NACP/alpha-synuclein-positive filamentous inclusions in astrocytes and oligodendrocytes of Parkinson's disease brains. *Acta Neuropathol.* **99**, 14–20.
- Wang, J., Vasaikar, S., Shi, Z., Greer, M., and Zhang, B. (2017). WebGestalt 2017: a more comprehensive, powerful, flexible and interactive gene set enrichment analysis toolkit. *Nucleic Acids Res.* **45**, W130–W137.
- Wichterle, H., Lieberam, I., Porter, J.A., and Jessell, T.M. (2002). Directed differentiation of embryonic stem cells into motor neurons. *Cell* **110**, 385–397.
- Wickham, H. (2009). *ggplot2: Elegant Graphics for Data Analysis* (Springer-Verlag, New York).
- Windrem, M.S., Osipovitch, M., Liu, Z., Bates, J., Chandler-Militello, D., Zou, L., Munir, J., Schanz, S., McCoy, K., Miller, R.H., et al. (2017). Human iPSC Glial Mouse Chimeras Reveal Glial Contributions to Schizophrenia. *Cell Stem Cell* **21**, 195–208.e6.
- Zhang, Y., Sloan, S.A., Clarke, L.E., Caneda, C., Plaza, C.A., Blumenthal, P.D., Vogel, H., Steinberg, G.K., Edwards, M.S., Li, G., et al. (2016). Purification and Characterization of Progenitor and Mature Human Astrocytes Reveals Transcriptional and Functional Differences with Mouse. *Neuron* **89**, 37–53.

STAR★METHODS

KEY RESOURCES TABLE

REAGENT or RESOURCE	SOURCE	IDENTIFIER
Antibodies		
Mouse anti-OCT4; 1:200	Millipore	Cat# MAB440; RRID:AB_358378
PE-conjugated mouse anti-human NANOG; 1:200	BD Biosciences	Cat# 560483; RRID:AB_1645522
Mouse anti-TRA-1-81; 1:200	Thermo Fisher Scientific	Cat# 41-1100; RRID:AB_2533495
PE-conjugated mouse anti-SSEA4; 1:200	Thermo Fisher Scientific	Cat# A14766; RRID:AB_2534281
Chicken anti-Sendai virus; 1:1000	Abcam	Cat# ab33988; RRID:AB_777877
Mouse anti-AFP; 1:200	Sigma-Aldrich	Cat# A8452; RRID:AB_258392
Mouse anti-SMA; 1:200	Sigma-Aldrich	Cat# A2547; RRID:AB_476701
Mouse anti-B-III-Tub; 1:2000	Sigma-Aldrich	Cat# T8660; RRID:AB_477590
Rabbit anti-LMX1a; 1:500	Abcam	Cat# ab139726; RRID:AB_2827684
Goat anti-FOXA2; 1:250	Santa Cruz	Cat# sc6554; RRID:AB_2262810
Donkey anti-mouse Alexa Fluor® 488; 1:400	Molecular Probes	Cat# A-21202; RRID:AB_141607
Donkey anti-chicken Alexa Fluor® 488; 1:400	Jackson Immuno Research Labs	Cat# 703-545-155; RRID:AB_2340375
Donkey anti-mouse Alexa Fluor® 555; 1:400	Thermo Fisher Scientific	Cat# A-31570; RRID:AB_2536180
Donkey anti-rabbit Alexa Fluor® 555; 1:400	Thermo Fisher Scientific	Cat# A31572; RRID:AB_162543
Donkey anti-mouse Alexa Fluor® 647; 1:400	Thermo Fisher Scientific	Cat# A31571; RRID:AB_162542
Donkey anti-rabbit Alexa Fluor® 647; 1:400	Thermo Fisher Scientific	Cat# A31573; RRID:AB_2536183
Donkey anti-goat Alexa Fluor® 555; 1:400	Thermo Fisher Scientific	Cat# A21432; RRID:AB_2535853
Rabbit anti-GFAP; 1:100	DAKO Cytomations	Cat# Z0334; RRID:AB_10013382
Mouse anti-S100b; 1:500	Sigma-Aldrich	Cat# S-2532; RRID:AB_477499
Rabbit anti-EZRIN; 1:500	Cell Signaling	Cat# 3145S; RRID:AB_2100309
Mouse anti-EAAT2; 1:500	Gift from Prof. Jeffrey Rothstein at Johns Hopkins.	N/A
Rabbit anti-AQP4; 1:500	Santa Cruz	Cat# sc-20812; RRID:AB_2274338
Mouse anti-GS; 1:500	Millipore	Cat# MAB-302; RRID:AB_2110656
Rabbit anti-ID3; 1:500	Cell Signaling	Cat# 9837S; RRID:AB_2732885
Rabbit anti-NF1A; 1:500	Active Motif	Cat# 39036; RRID:AB_2335600
Rabbit anti-SOX9; 1:500	Cell Signaling	Cat# 82630; RRID:AB_2665492
Rabbit anti-GM130; 1:200	Abcam	Cat# ab52649; RRID:AB_880266
Mouse anti-NF-kB; 1:800	Cell Signaling	Cat# 6956; RRID:AB_10828935
Mouse anti-HLA-DPb1; 1:500	Abcam	Cat# ab55152; RRID:AB_944199
Mouse anti-human HLA-DR, DP, DQ; 1:100	Biolegend	Cat# 361706; RRID:AB_2563192
Mouse anti-O4; 1:100	Gift from Prof. James E. Goldman at Columbia University of N.Y., USA	N/A
Human TruStain FcX; 1:100	Biolegend	Cat# 422302; RRID:AB_2818986
Rabbit anti-LAMP2A; 1:500	Abcam	Cat# ab18528; RRID:AB_775981
Mouse anti MHCII beta chain HLA-DPB1; 1:1000	Abcam	Ab55152
Goat anti-mouse IgG-HRP; 1:5000	Invitrogen	Cat# A28177
Bacterial and virus strains		
Retroviral vectors; References 1, 2, 3		
Sendai CytoTune-iPS 2.0; Thermo Fisher Scientific; Cat# A16517		

(Continued on next page)

REAGENT or RESOURCE	SOURCE	IDENTIFIER
Continued		
Chemicals, peptides, and recombinant proteins		
α SYN species, used at 10 μ M, frozen and stored at -80°C until use	CEA and Laboratory of Neurodegenerative Diseases	N/A
TNF α , used at 100 ng/ml	PeproTech	Cat# AF-300-01A
FGF2	Thermo Fisher Scientific	Cat# PHG0263
LDN	Stemgent	Cat# 04-0074-10
SB	Selleckchem	Cat# S1067
SHH-C25II	Thermo Fisher Scientific	Cat# PMC8034
CHIR	Sigma-Aldrich	Cat# SML1046
SAG	Millipore	Cat# 566660
FGF8b	Millipore	Cat# PHG0273
EGF	Peptidech	Cat# AF-100-15
Mouse laminin	Thermo Fisher Scientific	Cat# 23017-015
CNTF	R&D Systems	Cat# 450-13
ATTO-488	Atto-Tec GmbH	Cat# AD 488-35
ATTO-555	Atto-Tec GmbH	Cat# AD 550-35
ECL Femo	Thermo Fisher Scientific	Cat# 34096
Streptavidin Magnetic Beads	Thermo Fisher Scientific	Cat# 88816
Trypsin Gold	Promega	Cat# V5280
EZ-Link-Sulfo-NHS-S-S-Biotin	Thermo Fisher Scientific	Cat# 2133
Seahorse XF calibrant	Agilent	Cat# 100840-000
Seahorse XF-base medium	Agilent	Cat# 103334-100
M-PER extraction reagent	Thermo Fisher Scientific	Cat# 78501
DAPI; 1:10,000	Life Technologies	Cat# 62248
7-Aminoactinomycin D (7AAD)	BD Bioscience	Cat# 559925
Critical commercial assays		
Fast SYBR Green Cells-to-Ct kit	Thermo Fisher Scientific	Cat# 4402956
TaqMan Fast Advanced Master Mix	Thermo Fisher Scientific	Cat# 4444558
Pierce TM BCA assay	Thermo Fisher Scientific	Cat# 23227
Human Proinflammatory Panel I	MesoScale Discovery	Cat# K15049D
EZ-Link-Sulfo-NHS-S-S-Biotin	Thermo Fisher Scientific	Cat# 2133
Protein Assay Kit II	Bio-Rad	Cat# 500-0002
Citrate Synthase Kit	Sigma-Aldrich	Cat# CS0720-1KT
Clariom S array	Thermo Fisher Scientific	Cat# 902927
RNeasy Micro Kit	QIAGEN	Cat# 74004
Deposited data		
Gene expression microarray data	This study; in supplementary material, as well as at the Roybon laboratory website, section "Resources"	https://www.ipsc-cns-disease.lu.se/ipsc-laboratory-for-cns-disease-modeling/resources
Experimental models: cell lines		
Irradiated mouse embryonic fibroblasts feeder cells (CF1)	Thermo Fisher Scientific	Cat# A34181
Human induced pluripotent stem cell lines: CSC-9A, CSC-10A/B/C, CSC-7A/B, CSC-21B, CSC-18A, CSC19A, CSC-3G/S.	Reference 1, 2, 3; Roybon laboratory at Lund University, Sweden	N/A
Human induced pluripotent stem cell lines: CSC-36D, CSC-37R, CSC-28N, CSC-26B and CSC-27I/K	This study; Roybon laboratory at Lund University, Sweden	N/A

(Continued on next page)

Continued

REAGENT or RESOURCE	SOURCE	IDENTIFIER
Oligonucleotides		
TaqMan Primer GUSB	Thermo Fisher Scientific	Hs00939627_m1
TaqMan Primer RPL13A	Thermo Fisher Scientific	Hs04194366_g1
TaqMan Primer HSP90AB1	Thermo Fisher Scientific	Hs04194340_g1
TaqMan Primer HLA-DMA	Thermo Fisher Scientific	Hs00185435_m1
TaqMan Primer HLA-DRB1	Thermo Fisher Scientific	Hs04192464_mH
TaqMan Primer HLA-DPB1	Thermo Fisher Scientific	Hs03045105_m1
TaqMan Primer CXCL8	Thermo Fisher Scientific	Hs99999034_m1
TaqMan Primer HLA-F	Thermo Fisher Scientific	Hs04185703_gH
Software and algorithms		
FACSDiva v8.0	BD Biosciences	N/A
Prism 7	GraphPad	N/A
Canvas Draw 1.0	Canvas GFX	N/A
R	R Core Team, 2020	N/A
Microplate Manager 5.2.1	Bio-Rad	N/A
Metamorph	Molecular Devices	N/A
Other		
Olympus IX-73 inverted microscope	Olympus	N/A
Leica TCS SP8 confocal microscope	Leica	N/A
C18 Aurora UHPLC column with CSI fittings	Ion Opticks (250mm X 75 μ m)	Cat# AUR2-15075C18A-CSI
Seahorse XFe96 analyzer	Agilent	N/A
BD FACSAria III	BD Biosciences	N/A
Ultrasonic processor UIS250v	Hielscher Ultrasonic	N/A
Microplate reader Model 680	Bio-Rad	N/A
iMark Microplate reader	Bio-Rad	N/A
Nano LC and Mass Spectrometer	EASY-nLC II high performance liquid chromatography (HPLC) system (Proxeon, ThermoScientific, Waltham, MA) coupled to the nanoElute tims TOF Pro (Bruker) Separation column: C18 Aurora UHPLC with CSI fittings (250mm X 75 μ m, Ion Opticks)	N/A

RESOURCE AVAILABILITY

Lead contact

Further information and requests for resources and reagents should be directed to the Lead Contact, Laurent Roybon (laurent.roybon@med.lu.se).

Materials availability

iPSC lines generated in this study are biobanked at the CSC Laboratory, at Lund University, Sweden.

Data and code availability

Microarray and proteomic data are available in [Tables S1](#), [S2](#), and [S3](#), as well as at the Roybon laboratory website (<https://www.ipsc-cns-disease.lu.se/ipsc-laboratory-for-cns-disease-modeling/resources>). Affymetrix data can be found at NCBI with GSE reference series number: GSE166771 (<https://www.ncbi.nlm.nih.gov/geo/query/acc.cgi?acc=GSE166771>).

EXPERIMENTAL MODEL AND SUBJECT DETAILS

Ethics

All patient biopsies that served to generate the iPSCs were obtained with informed consent and after ethical committee approval at the Parkinson institute in Milan, Italy: Ethics Committee “Milano Area C” (<https://comitatoeticoareac.ospedaleniguarda.it/>) on the 26/06/2015, and registered under the number: 370-062015. The samples were expanded to generate fibroblasts cell lines and stored at the Telethon genetic biobank (<http://biobanknetwork.telethon.it/Pages/View/Documents>). The reprogramming of patient samples was regulated by a permit delivered to Dr. Laurent Roybon by the Swedish work environment authority and registered under the number 2020-3211. Work was carried out according to European and Swedish national rules, with the highest level of ethics.

iPSC line derivation and production of astrocytes

iPSC generation for CSC-9A, CSC-10A/B/C, CSC-7A/B, CSC-21B, CSC-18A, CSC-19A, and CSC-3G/S was previously published (Holmqvist et al., 2016). The same procedure was used to reprogram human epidermal fibroblasts, harvested using a skin punch biopsy from healthy donors CSC-36D and CSC-37R (Pomeshchik et al., 2020), a PD patient with a *SNCA* gene triplication CSC-28N (parent fibroblasts were previously employed to generate the lines CSC-3G and -3S), and two PD patients with idiopathic PD CSC-26B (59 year old female) and CSC-27I/K (47 year old male).

In this study, astrocytes were generated from 74 differentiations in total, all started from pluripotent stem cell stage, from 17 iPSC clones (2-3 clones per donor group) generated from 9 familial and idiopathic PD patients, and 2 healthy individuals. iPSCs were differentiated using a midbrain patterning sequence and expanded as embryoid bodies followed by astrocyte differentiation, expansion, and maturation in adherent cultures to generate mature astrocytes following the outline in Figure 1C. As opposed to previous work (Holmqvist et al., 2015; Roybon et al., 2013), we used a serum-free differentiation protocol as serum exposure may alter the morphology and transcriptome (Pekny and Pekna, 2016; Sloan et al., 2017).

METHOD DETAILS

iPSC generation

Briefly, donor fibroblasts were cultured and expanded in Dulbecco’s modified eagle’s medium (DMEM) supplemented with 10% fetal bovine serum and 1% penicillin-streptomycin (P/S; v/v) at 37°C and 5% CO₂ for several passages before being cryopreserved in liquid nitrogen and stored at –150°C. Donor fibroblasts (75,000 cells/well) were plated on 0.1% gelatin-coated 12-well plate and after two days at 37°C at 5% CO₂, reprogrammed by use of either retrovirus or non-integration Sendai virus (CytoTune-iPS 2.0) to deliver the reprogramming genes *OCT3/4*, *SOX2*, *cMYC*, and *KLF4*. After 7 days of culture, cells were passaged and seeded on irradiated mouse embryonic fibroblasts feeder cells (CF-1 MEF, GlobalStem) with WiCell media composed of advanced DMEM-F12, 20% Knock-Out Serum Replacement (v/v), 2 mM L-glutamine (L-Glu), 1% non-essential amino acids (NEAA; v/v; Millipore), 0.1 mM β-mercaptoethanol (Sigma-Aldrich), and 20 ng/ml FGF2. After 28 days, several clones were isolated and selected based on the morphology of the colonies and seeded onto a MEF-coated 12-well plate with media changed daily and further characterized. The generated lines stained positive for the common nuclear and cell surface pluripotency markers, *OCT3/4*, *NANOG*, and *TRA1-81* (Figure S1). An alkaline phosphatase (AP) staining was done using the AP staining kit according to manufacturer’s protocol (Stemgent), which further confirmed the pluripotency of the iPSC lines (Figure S1). All lines had normal karyotype following a G-banding analysis at 300–400 band resolution on average when testing between passages 8–15 at the Department of Clinical Genetics and Pathology in Lund (Figure S1). All lines were cleared of Sendai virus when tested between passages 8–15 (Figure S1). Genetic integrity was confirmed by fingerprint analysis of isolated DNA from the donor fibroblasts and their respective iPSC line (IdentiCell STR profiling service; Department of Molecular Medicine, Aarhus University Hospital, Denmark). DNA was isolated for direct sequencing using a lysis buffer (100 mM Tris (pH 8.0), 200 mM NaCl, 5 mM EDTA, and 0.2% SDS in distilled and autoclaved water supplemented with 1.5 mg/ml Proteinase K). The presence of the *SNCA* triplication was previously confirmed in our iPSC library study. Lastly, all lines were cultured as EBs and plated on a 96-well plate to demonstrate their ability to spontaneously differentiate into the three germ layers, which was confirmed using immunofluorescent staining with antibodies against B-III-tubulin (B-III-tub), smooth muscle actin (SMA), and α-fetoprotein (AFP; Figure S1).

Differentiation of iPSCs to astrocytes

On day one of differentiation, human iPSC colonies were harvested, dissociated, filtered (100 μm), and added to an ultra-low-adherent flask (Sigma-Aldrich) with 0.1 μM LDN (Stemgent), 10 μM SB (Selleckchem), 200 ng/ml SHH-C25II (Thermo Fisher Scientific), 0.8 μM CHIR (Stemgent), and 1 μM SAG (Millipore) for 0–4 days in neural induction medium [NIM; advanced DMEM-F12 with 1% L-Glu, 1% NEAA, 1% N2, and 1% P/S (100 U/mL)]. From day 6–8 NIM with 0.1 μM LDN, 0.8 μM CHIR (Stemgent), and 2 μM SAG (Millipore) was used. On day 10, NIM with 0.8 μM CHIR (Stemgent) and 2 μM SAG (Millipore) were used. From days 12–30, NIM with 100 ng/ml FGF8b (Thermo Fisher Scientific) and 2 μM SAG (Millipore) was used. On day 30 EBs were dissociated, filter strained (100 μm), and transferred to a ultra-low-adherent flask containing neural expansion medium [(NEM; DMEM-F12 with 1% L-Glu, 1% NEAA, 2% B27 without vitamin A, 1% P/S, and 0.2 μg/ml heparin (Sigma-Aldrich)] with 20 ng/ml FGF2 (Thermo Fisher Scientific) and 20 ng/ml EGF (Peprotech) for 30 days. On day 60, EBs were washed and dissociated with 0.05% trypsin/1X-EDTA and seeded to

adherent culture flasks coated with 20 $\mu\text{g/ml}$ Poly-L-ornithine hydrobromide (P/O; Sigma-Aldrich) and mouse laminin (15 $\mu\text{g/ml}$ for initial seeding, then 5 $\mu\text{g/ml}$ for subsequently passages) containing NEM and 20 ng/ml CNTF (R&D Systems) for 60-80 days in NDM. Finally, from days 80-100, astrocytes were cultured in neural differentiation medium [NDM; (NB with 1% L-Glu, 1% NEAA, 1% N2, and 1% P/S) with and 20 ng/ml CNTF (R&D Systems)]. Cells were passaged at confluency. Media was changed every 2 days from day 0-30 and every 3-4 days from day 30-100.

αSYN purification and species preparation

The expression and purification of human wild-type (WT) αSYN was performed as previously described (Ghee et al., 2005). WT αSYN was incubated in buffer A (50 mM Tris-HCl, pH 7.5, 150 mM KCl) to obtain the fibrillar polymorph “fibrils,” in buffer B (5 mM Tris-HCl, pH 7.5) for “ribbons,” in buffer C (20 mM MES pH6.5, 150 mM NaCl) for “F65,” and in buffer D (20 mM KPO₄ pH9.1) for “F91,” at 37°C under continuous shaking in an Eppendorf Thermomixer set at 600 rpm for 4-7 days (Bousset et al., 2013; Makky et al., 2016). A truncated human αSYN spanning residues 1-110 was generated by introducing two stop codons after residue 110 by site directed mutagenesis. This variant was purified exactly as full-length αSYN and was assembled into fibrillar structures “F110” in buffer A. The fibrillar αSYN strains were centrifuged twice at 15,000 g for 10 min and re-suspended twice in PBS at 1.446 g/L. On-fibrillar assembly oligomeric αSYN in PBS was prepared as described (Pieri et al., 2016b). All preformed assemblies as well as monomeric αSYN in PBS were labeled with ATTO-488 (or ATTO-555) NHS-ester (Atto-Tec GmbH) fluorophore following the manufacturer’s instructions using a protein:dye ratio of 1:2. The labeling reactions were arrested by the addition of 1 mM Tris pH 7.5. For fibrillar assemblies, the unreacted fluorophore was removed by a cycle of two centrifugations at 15,000 g for 10 min followed by resuspension of the pellets in PBS. For monomeric and oligomeric αSYN , the unreacted dye was removed using a desalting column (PD10, GE Healthcare) equilibrated in PBS buffer, pH 7.4. The quality control of recombinant human WT αSYN monomeric, oligomeric, fibrillar polymorphs, and F110 was carried out as previously described (Bousset et al., 2013; Makky et al., 2016). For transmission electron microscopy, the assemblies were adsorbed on 200 mesh carbon-coated electron microscopy grids and imaged after negative staining. For fibrillar polymorph fingerprint analysis, aliquots of fibrillar assemblies were removed before or after addition of proteinase K, denatured in boiling Laemmli buffer for 5 min at 90°C, subjected to SDS-PAGE on 12% polyacrylamide gels, and stained by Coomassie coloration. Monomeric and oligomeric αSYN were analyzed by analytical ultracentrifugation (Pieri et al., 2016b). The fibrillar polymorphs were fragmented by sonication for 20 min in 2 mL Eppendorf tubes in a Vial Tweeter powered by an ultrasonic processor UIS250v (250 W, 2.4 kHz; Hielscher Ultrasonic, Germany) to generate fibrillar particles with an average size 42-52 nm.

Gene expression analysis

Day 97-105 astrocytes were seeded at 300,000 cells/well in a 6-well plate coated with 20 $\mu\text{g/ml}$ P/O (Sigma-Aldrich) and 5 $\mu\text{g/ml}$ mouse laminin for 2 days and treated with either PBS (referred to as non-treated in the study), 100 ng/ml TNF α , or 10 μM αSYN (monomers, fibrils, or F110) for 6 days. Astrocytes were then washed twice with PBS and frozen at -80°C before shipping to Kompetenz-zentrum Fluoreszente Bioanalytik (Germany) for gene expression analysis using the Clariom S array (Affymetrix). The total RNA was extracted from dry cells according to RNeasy Micro Kit protocol (QIAGEN). Sample preparation for microarray hybridization was carried out as described in the Affymetrix GeneChip WT PLUS Reagent Kit User Manual (Affymetrix). Summarized probe set signals in log₂ scale were calculated by using the GCCN-SST-RMA algorithm with the Affymetrix GeneChip Expression Console v1.4 Software. Average signal values, comparison of fold changes, and significance P values were calculated with R. Probe sets with a fold change above 4-fold (for TNF α -treated samples) and 1.5-fold (for αSYN -treated samples) and a Student’s t test P value lower than 0.05 were considered as significantly regulated.

Flow cytometry analysis

Day 97-105 astrocytes were seeded at 500,000 cells/well in a 24-well plate coated with 20 $\mu\text{g/ml}$ P/O (Sigma-Aldrich) and 5 $\mu\text{g/ml}$ mouse laminin for 2 days and treated with either PBS (non-treated), 100 ng/ml TNF α , 10 μM αSYN (monomers, fibrils, or F110), 10 μM αSYN fibril plus 100 ng/ml TNF α , or 10 μM αSYN F110 plus 100 ng/ml TNF α for 6 days. Astrocytes were dissociated using pre-wared Accutase and re-suspended in neural differentiation medium without phenol red. Cells were blocked with 5% donkey serum and TruStain FcX (1:100) for 10 min at RT and then stained for human HLA-DR, DP, DQ (1:100). 7-Aminoactinomycin D (7AAD) was added to detect dead cells and incubated on ice for 5 min prior to analysis. Samples were analyzed using a BD FACSAria III (BD Biosciences) with FACSDiva v8.0 software (BD Biosciences) at the MultiPark Cellomics and Flow Cytometry Core technical platform at Lund University. The cytometer was set up using a 100 μm nozzle at standard pressure of 20 psi and a frequency of 30.0 kHz and was calibrated daily using BD FACSDiva Cytometer Setup and Tracking (CS&T) software and CS&T Research Beads (BD Biosciences). 7-7AAD was excited by the blue laser (488 nm/20 mW) and emission was detected through a 695/40 bandpass (BP) filter. FITC was excited by the yellow/green laser (561 nm/50 mW); emission at 610/20 BP. The strategy for gating was set to separate live and dead cells based on uptake of 7-AAD (data not shown) and FITC-positive cells compared to unstained astrocytes for each treatment condition. Each analysis was based on 10,000 to 20,000 events.

Quantitative RT-PCR

Day 100-105 old astrocytes were seeded at 18,000 cells/well in a 96-well plate coated with 20 $\mu\text{g/ml}$ P/O (Sigma-Aldrich) and 5 $\mu\text{g/ml}$ mouse laminin for 2 days and treated with either PBS (non-treated), 100 ng/ml TNF α , 10 μM αSYN (monomers, fibrils, or F110), 10 μM

α SYN fibril plus 100 ng/ml TNF α , or 10 μ M α SYN F110 plus 100 ng/ml TNF α for 1 or 6 days. Fast SYBR Green Cells-to-Ct kit (Ambion) was used for lysis of astrocytes and reverse transcription to cDNA. The qRT-PCR was done with TaqMan Fast Advanced Master Mix and TaqMan primers (both from Thermo Fisher Scientific) and run according to the manufacturer's protocol. C_T-values were normalized to the geometric mean of the housekeeping genes *Hsp90AB1*, *GUSB* and *RPL13A* using the $\Delta\Delta$ C_T-method. Results were shown as fold change to mean of non-treated samples and a one-way ANOVA with a *P* value of < 0.05 was considered significant. Primer ID list and catalog numbers: *GUSB* (Hs00939627_m1); *RPL13A* (Hs04194366_g1); *HSP90AB1* (Hs04194340_g1); *HLA-DMA* (Hs00185435_m1); *HLA-DRB1* (Hs04192464_mH); *HLA-DPB1* (Hs03045105_m1); *CXCL8* (Hs99999034_m1); *GOLGA8B* (Hs00367259_m1); *LONP1* (Hs00998407_m1); *DNM1L* (Hs01552605_m1); *HLA-F* (Hs04185703_gH).

Pro-inflammatory cytokine analysis

Day 97-105 astrocytes were seeded at 20,000 cells/well in a 96-well plate coated with 20 μ g/ml P/O (Sigma-Aldrich) and 5 μ g/ml mouse laminin for 2 days and treated with either PBS, 100 ng/ml TNF α , or 10 μ M α SYN (monomers, fibrils, or F110) for 1 hour, 24 hours and 6 days with growth media collected and frozen at -80°C until analyzed. Total protein was determined immediately after growth media was removed and plates for immunocytochemical analysis were immediately fixed (see section below). Total protein from the cell pellet was determined using the PierceTM BCA assay. M-PERTM extraction reagent was used to lyse cells and the BCA assay was run according to the manufacturer's specified protocol using BSA as a standard and Milli-Q water as blank. Protein samples were analyzed and used to normalize cytokine concentrations. Growth media from astrocytes was quantified using the multiplex pro-inflammatory Panel I (MesoScale Discovery, USA), an electrochemiluminescence sandwich immune-assay, for 10 cytokines including: IFN- γ , IL-1 β , IL-2, IL-4, IL-6, IL-8, IL-10, IL-12p70, IL-13, and TNF α . Samples were diluted 1:1 in supplied buffer and analyzed in duplicates according to the manufacturer's specified protocol. Concentrations were normalized using total protein (pg/ μ g protein). Samples below or above the sensitivity of the assay were set to zero or the max value, respectively. Out of 69 experiments performed, 3 failed and were not included in the analysis (one for GBA, PARK2, and SNCA), as the value for non-treated astrocytes was similar or above that obtained for TNF α -treated astrocytes, which was close to or above the max value of the assay.

Immunocytochemical analysis

Cell cultures were fixed with 4% paraformaldehyde for 10 min at RT followed by standard immunocytochemical procedures, 1 hour, 24 hours and 6 days post-treatment. Blocking was done in 10% donkey serum in PBS with 0.1% Triton X-100 (Sigma-Aldrich) for 1 h at RT. Primary antibodies, listed below, were added to the wells and incubated overnight at 4°C . Next the secondary antibodies, listed below, were added and incubated for 1h at RT in the dark. Additionally, nuclei were stained by DAPI (1:10,000; Life Technologies). All fluorescent photomicrographs were taken using an inverted epifluorescence microscope (LRI – Olympus IX-73) or confocal microscope (Leica TCS SP8 confocal microscope (Leica Microsystems) equipped with diode 405/405 nm and argon (405, 488, 552, 638 nm) lasers with a HP PL APO 63x/NA1.2 water immersion objective). EBs were taken at day 15 for analysis. They were fixed, sectioned and stained as previously described (Wichterle et al., 2002).

Pull-down assay and mass spectrometry

Ten million astrocytes were exposed or not to α SYN fibrils labeled with biotin (10 μ M) for 6 days. α SYN fibrils in PBS were labeled by addition of 2 molar equivalents of EZ-Link-Sulfo-NHS-S-S-Biotin (Thermo Fisher Scientific #2133) for 1 h at room temperature. The reaction was stopped by addition of Tris-HCl buffer pH 7.5 to a final concentration of 40 mM and incubation during 10 min. The biotinylated α SYN fibrils were recovered by centrifugation, 30 min at 25,000 g at room temperature and resuspended in PBS. The astrocytes were scraped and cytosol and membrane fractions were prepared by incubating the cells with 0.015% digitonin and separating the two fractions by centrifugation (500 g) for 5 min at room temperature. Pull-down experiments were performed on cytosolic and membrane fractions of astrocytes exposed or not to biotinylated α SYN fibrils using streptavidin beads. The presence of MHC-class II proteins within the pull-down was assessed by western blot analysis after PAGE (12% acrylamide) and transfer to nitrocellulose membranes, using the anti-MHC-II beta chain HLA-DP β 1 mouse antibody, the anti-mouse secondary IgG-HRP goat antibody, and ECL Femto (Pierce, Waltham, MA). For mass spectrometry analysis, 250 μ g of astrocyte (exposed to biotin labeled α SYN fibrils or not) membrane proteins were loaded onto 90 μ l of magnetic beads functionalized with streptavidin (Pierce, Waltham, MA). The pulled down proteins were eluted by 50 μ l of Laemmli denaturing buffer, subjected to PAGE and in-gel digested with trypsin Gold (Promega) at a concentration of 10 ng/ μ l in 25 mM ammonium bicarbonate. The tryptic peptides were dried and resuspended in 10 μ l 0.1% trifluoroacetic acid, desalted using a zip-tip C18, eluted, dried and resuspended in TFA. 1 μ l, corresponding to 250 ng of total proteins, and an equivalent of 1 μ g of proteins were loaded on the streptavidin beads for the pulled-down fractions were loaded on an C18 Aurora UHPLC column with CSI fittings and the peptides were eluted with a 100 min gradient.

Seahorse analysis

Mitochondrial respiration was analyzed using the Seahorse XF96 analyzer (Agilent) following the manufacturer's instructions. Briefly, at day minus 9 (–9), 96-well seahorse plates (Agilent) were coated with P/O (20 μ g/ml; Sigma-Aldrich) and mouse laminin (5 μ g/ml). At day –8, 95-100-day astrocytes were seeded (30,000 cells/well) in 80 μ L of NDM with CNTF (20 ng/ml; R&D Systems). At day –6, media was changed and NDM added and cells were either left untreated (PBS condition) or treated with TNF α (100 ng/ml) or α SYN monomers, fibrils, or F110 (10 μ M). At day –1, Seahorse XF calibrant (Agilent) was added to hydrate the sensor cartridge

and incubated at 37°C in a CO₂-free incubator (Agilent). On the day of the experiment, XF-base medium (Agilent) was supplemented with 5 mM pyruvate (Sigma-Aldrich), 2 mM L-glutamine (Thermo Fisher Scientific), and 10 mM glucose (Sigma-Aldrich) and adjusted to pH 7.4 at 37°C. Cells were washed in XF-base medium (Agilent) and left in a non-ventilated, non-CO₂ incubator at 37°C for at least an hour. Oxygen consumption rate (OCR) was measured at baseline (basal) and after sequential additions of 1 μg/ml oligomycin (to inhibit ATP synthase (complex V); measure of coupled respiration), 1 μM FCCP (to uncouple oxygen consumption from ATP production; measure of maximal respiration), and 2 μM rotenone (to inhibit complex I) and 1 μg/ml antimycin A (to inhibit complex III; measure of nonmitochondrial respiration). The FCCP concentration used to measure maximal uncoupled OCR has been determined in a separate set of experiments (data not shown). The average of all data points per respiratory state was used for statistical analysis with exception of FCCP where the data point showing the highest OCR was selected. Following the measurements, the medium was removed and the plate washed with PBS and either PBS or M-PER™ extraction reagent was added to the cells before storage at –20°C for total protein or citrate synthase activity measurements, respectively. The total protein was determined according to the manufacturer's instructions using the Protein Assay Kit II (Bio-Rad) with BSA standard (Bio-Rad) and Milli-Q H₂O as blank. Samples were analyzed and used to normalize Seahorse oxygen consumption rate (OCR). Citrate synthase was determined according to the manufacturer's instructions using a Citrate Synthase Kit (Sigma-Aldrich). Briefly, sample reagent mix was added to each well of the XFe-96 Seahorse plate (Agilent) and the entire well content was transferred to a 96-well plate. Reagent Mix was added to control and samples and background was measured. 10 mM Oxaloacetate Solution was added and citrate synthase activity was determined using a microplate reader. Citrate synthase activity below 1 μmol/ml/min was reanalyzed and if still below 1 μmol/ml/min excluded from the technical replicates. Background values were removed from final measurements. Seahorse analysis was performed with 8 technical replicates from 2 biological replicates. Wells that did not respond to the addition of the drugs were removed from analysis. OCR values were corrected for non-mitochondrial oxygen consumption using the antimycin values. Coupled respiration (respiration linked to phosphorylation by the ATP-synthase) was determined by subtracting the oligomycin OCR from the basal OCR. All values were normalized using citrate synthase activity to show respiratory changes corrected for differences in mitochondrial content of the cells (OCR per CS activity; [pmol O₂ min⁻¹ / μmol/ml/min]) and displayed as a percent of NT.

QUANTIFICATION AND STATISTICAL ANALYSIS

Statistics

Statistical analyses were performed either with GraphPad Prism 7 software or with R (<https://www.r-project.org/>). Data were presented as mean ± s.e.m. A P value of < 0.05 was considered significant. * p ≤ 0.05; ** p ≤ 0.01, *** p ≤ 0.001, **** p ≤ 0.0001. For the cytokine analysis, 2-3 biologically independent clones with 2-5 differentiations per clone (indicated in the figure or legend) were used. An ANOVA with Dunnett's or Tukey post-test was performed if there were multiple treatment comparisons and time points. A Student's t test was used when comparing a treatment group to the control for the FACS and seahorse experiments.

Aggregate size counting

The length of the aggregates was measured using the Metamorph software tool "box measurement tool," which produced pixel values that were then converted into length in μm. A total of 75 random ATTO-positive aggregates were counted.

Bioinformatics

Microarray data handling and analyses were performed using R. We used the gene symbol identifiers of the probes in the gene expression datasets to retain those genes for which there was an Entrez gene identifier using the org.Hs.eg.db package version 3.11.4 available via bioconductor/R, a collaborative open source statistical programming environment (Gentleman et al., 2004). The p value of the filtered data was adjusted for multiple comparison by performing the Benjamini-Hochberg false discovery rate calculation in R. We flagged as significant genes for which the raw p values (sig_p value) were less than 0.05 and less than the corresponding adjusted p value, as previously employed by Windrem and colleagues (Windrem et al., 2017). Heatmaps of gene expression and fold change between condition versus PBS-treated astrocytes were made with ComplexHeatmap version 2.4.3 (Gu et al., 2016). Volcano plots of log P value against log fold change were done using ggplot2 version 3.3.0 (Wickham, 2009). KEGG pathway analysis was performed with WebGestalt version 0.4.4. (Wang et al., 2017).